Journal of Theoretical Biology 266 (2010) 307–322

Contents lists available at ScienceDirect

Journal of Theoretical Biology

journal homepage: www.elsevier.com/locate/yjtbi

Lifelong dynamics of human $CD4^+CD25^+$ regulatory T cells: Insights from *in vivo* data and mathematical modeling

Irina Baltcheva [a,1,*], Laura Codarri [b,1,2], Giuseppe Pantaleo [b], Jean-Yves Le Boudec [a]

[a] Laboratory for Computer Communications and Applications, École Polytechnique Fédérale de Lausanne, EPFL IC-LCA, Batiment BC 258, Station 14, CH-1015 Lausanne, Switzerland
[b] Laboratory of AIDS Immunopathogenesis, Division of Immunology and Allergy, Department of Medicine, Centre Hospitalier Universitaire Vaudois, University of Lausanne, Switzerland

ARTICLE INFO

Article history:
Received 2 August 2009
Received in revised form
14 June 2010
Accepted 15 June 2010
Available online 22 July 2010

Keywords:
Mathematical model
Regulatory T cells
Lifelong *in vivo* dynamics
Maximum likelihood estimation

ABSTRACT

Despite their limited proliferation capacity, regulatory T cells (T_{regs}) constitute a population maintained over the entire lifetime of a human organism. The means by which T_{regs} sustain a stable pool *in vivo* are controversial. Using a mathematical model, we address this issue by evaluating several biological scenarios of the origins and the proliferation capacity of two subsets of T_{regs}: precursor $CD4^+CD25^+CD45RO^-$ and mature $CD4^+CD25^+CD45RO^+$ cells. The lifelong dynamics of T_{regs} are described by a set of ordinary differential equations, driven by a stochastic process representing the major immune reactions involving these cells. The model dynamics are validated using data from human donors of different ages. Analysis of the data led to the identification of two properties of the dynamics: (1) the equilibrium in the $CD4^+CD25^+FoxP3^+T_{regs}$ population is maintained over both precursor and mature T_{regs} pools together, and (2) the ratio between precursor and mature T_{regs} is inverted in the early years of adulthood. Then, using the model, we identified three biologically relevant scenarios that have the above properties: (1) the unique source of mature T_{regs} is the antigen-driven differentiation of precursors that acquire the mature profile in the periphery and the proliferation of T_{regs} is essential for the development and the maintenance of the pool; there exist other sources of mature T_{regs}, such as (2) a homeostatic density-dependent regulation or (3) thymus- or effector-derived T_{regs}, and in both cases, antigen-induced proliferation is not necessary for the development of a stable pool of T_{regs}. This is the first time that a mathematical model built to describe the *in vivo* dynamics of regulatory T cells is validated using human data. The application of this model provides an invaluable tool in estimating the amount of regulatory T cells as a function of time in the blood of patients that received a solid organ transplant or are suffering from an autoimmune disease.

1. Introduction

Regulatory T cells (T_{regs}) are important in the adaptive immune system. They act as antagonists to immune responses by suppressing the activation and proliferation of $CD4^+$ helper and $CD8^+$ killer T cells. By this means, they are involved in self-tolerance (Kim et al., 2007), homeostasis and in the control of excessive immune reactions. They are identified by the surface expression of CD4, as well as by high levels of CD25, the alpha-chain of the interleukin-2 (IL-2) receptor (Sakaguchi et al., 1995). In addition, they express the forkhead/winged-helix transcription factor FoxP3 (Fontenot et al., 2003; Hori et al., 2003), a negative modulator of IL-2 transcription and are therefore referenced as $CD4^+CD25^+FoxP3^+$ T_{regs}. Several other markers have been associated with T_{regs}, notably high levels of CTLA-4 (cytotoxic T-lymphocyte associated molecule-4), CD62L, CCR7, GITR (glucocorticoid-induced TNF receptor) and low levels of CD127 (the alpha-chain of the IL-7 receptor) (Codarri et al., 2007; Liu et al., 2006; Seddiki et al., 2006a). It has been shown that T_{regs} are unable to produce themselves the growth factor IL-2 (Jonuleit et al., 2001) and their proliferation in case of inflammation is dependent on other IL-2 producers (typically $CD4^+CD25^-$ T cells). Moreover, T_{regs} are difficult to activate through their T cell receptor and require optimal stimulation conditions in order to initiate a clonal expansion (Takahashi et al., 1998).

As of today, two developmental pathways of human regulatory T cells *in vivo* have been identified (Sakaguchi, 2003): naturally occurring thymus-derived T_{regs} (Wing et al., 2002; Seddiki et al., 2006b; Hoffmann et al., 2006; Fritzsching et al., 2006) and adaptive or induced T_{regs}, derived from non-regulatory $CD4^+$

* Corresponding author. Tel.: +41 21 693 1266.
E-mail address: irina.baltcheva@gmail.com (I. Baltcheva).
[1] The first two authors contributed equally to this study.
[2] Present address: Institue of Experimental Immunology, University of Zürich, Switzerland.

0022-5193/$ - see front matter © 2010 Elsevier Ltd. All rights reserved.
doi:10.1016/j.jtbi.2010.06.024

$CD25^-FoxP3^-$ T cells (Walker et al., 2003; Kretschmer et al., 2005; Vukmanovic-Stejic et al., 2006). Naturally occurring T_{regs} originate in the thymus and are released in the periphery with a naive phenotype (Seddiki et al., 2006b; Cupedo et al., 2005; Takahata et al., 2004; Wing et al., 2003, 2002). They are identified as $CD4^+CD25^+CD45RO^-$ T cells and will be called "precursor" T_{regs} throughout this article. Once precursors encounter their cognate antigen, they acquire a suppressive capacity and a memory phenotype (Fritzsching et al., 2006). We call these differentiated cells "mature" T_{regs}. Adaptive T_{regs} are derived from rapidly proliferating activated-effector or memory $CD4^+CD25^-$ T cells that acquire the permanent expression of CD25 and the suppressive function in the periphery (Walker et al., 2003; Vukmanovic-Stejic et al., 2006). Because they have experienced antigen, these cells have a mature profile and express the memory phenotype CD45RO. It is important to remark that there is no difference regarding the surface markers characterizing both types of mature T_{regs} and consequently, one cannot distinguish both T_{regs} origins using fluorescent techniques. The same observation can be made about T-cell receptor excision circles (TREC): T_{regs} from both origins have similar decreased TREC content (Kasow et al., 2004). Thymus-derived regulatory cells divide during clonal selection in the thymus and in the periphery, whereas activation-induced regulatory cells come from rapidly proliferating non-regulatory T cells and therefore have decreased TREC content.

In vivo studies of human T_{regs} have shown that the number of precursors decreases significantly with age (Seddiki et al., 2006b; Valmori et al., 2005), whereas the number of mature T_{regs} increases in elderly individuals (Gregg et al., 2005). Thymic involution, together with the fact that $CD4^+CD25^+CD45RO^+$ mature regulatory T cells are known to be non-proliferating, introduces the question of how is developed and maintained a stable pool of T_{regs} throughout life. Different hypotheses are evoked in Akbar's opinion paper (Akbar et al., 2007); the question of proliferation is central. The first hypothesis claims that precursor $CD4^+CD25^+CD45RO^-$ cells are able to proliferate (Walker et al., 2003; Klein et al., 2003) and even though the thymic involution reduces the input of newly produced precursors with age, these cells are the main reservoir of mature T_{regs}. The second hypothesis suggests that both precursor and mature T_{regs} are non-proliferating but although mature T_{regs} are sensitive to death because of their high levels of CD95 (Fritzsching et al., 2006; Taams et al., 2001), the fact that precursors are apoptosis-resistant suffices to sustain a stable pool of mature T_{regs}. Finally, the third hypothesis points out the presence of an external source of mature T_{regs}, derived from rapidly proliferating effector $CD4^+CD25^-$ T cells (Taams et al., 2001; Vukmanovic-Stejic et al., 2006). Thus, there is a controversy about the mechanisms by which T_{regs} regenerate throughout the lifetime of individuals. The objective of our study is to evaluate the above biological hypotheses by the means of a mathematical model and to measure their effect on the development and maintenance of a pool of human T_{regs}.

A major difficulty encountered in mathematical modeling of biological systems is dealing with parameter values. The more detailed the model is, the more parameters it involves and its behavior can be completely different according to the values taken by the latter. Good parameter estimates exist in some cases, but it is often difficult to build an experiment that allows for their direct measurement. In the mathematical model presented hereafter, we employ a modeling technique that alleviates the parameter estimation problem by considering parameters as random variables having *a priori* distributions (as in Bayesian approaches). This approach allows us to evaluate simultaneously several values, to produce results that depend little on the exact values, and therefore to diminish the probability of errors due to wrong parameter estimates.

Using the above technique, we define a generic model describing the lifelong dynamics of T_{regs}. We attempt to include in it all the actual knowledge about the population dynamics of regulatory T cells, while keeping the model as simple as possible. We consider all events that affect the population size of T_{regs}: immune reactions to self- or foreign antigens, the homeostatic activity and the external input—from the thymus or from the non-regulatory effector $CD4^+CD25^-$ T cell pool. We then implement the above-mentioned hypotheses about the origins and proliferation capacity of T_{regs}. In order to validate the model, we compare it to human data consisting in measurements of T_{regs} as a function of age. We first study the expected model behavior where the stochastic parameters take the average value of their *a priori* distributions. Then, we evaluate the performance of the model with random parameters. Its behavior is evaluated for several values inside the given parameter range and the density of trajectories is estimated. This density leads to the definition of the likelihood of a model scenario, used to formally reject the scenarios that are unable to fit the data.

Analysis of the *in vivo* data indicates that homeostasis is maintained over both $CD4^+CD25^+CD45RO^-$ and $CD4^+CD25^+CD45RO^+$ populations taken together and that the ratio between $CD4^+CD25^+CD45RO^-$ precursor and $CD4^+$ $CD25^+CD45RO^+$ mature T_{regs} is inverted in the first years of adulthood. Following our mathematical analysis, we claim that one of the following conclusions must be true: if there is a homeostatic regulation of the mature T_{regs} population or there is a thymic or external input of mature T_{regs}, the antigen-driven proliferation of precursor or of mature T_{regs} is *not* necessary for the development and maintenance of a pool of T_{regs}. However, in the absence of a density-dependent homeostasis mechanism or of an external contribution to the mature T_{regs} population, the antigen-driven proliferation of precursors in the periphery is needed for the development and the maintenance of the pool of mature T_{regs}.

2. Materials and methods

2.1. Immunological data

2.1.1. Biological specimens

A transversal study was performed on the peripheral blood of 120 healthy subjects constituted by 60 males with a median age of 52.6 (range 20–81) and 60 females with a median age of 49.32 (range 19–78). Samples of peripheral blood were obtained from laboratory co-workers or from the Blood Bank of the Centre Hospitalier Universitaire Vaudois, University of Lausanne, while the seven samples of cord blood and the two thymuses were obtained from the Department of Clinical Chemistry, Microbiology and Immunology, University Hospital, University of Ghent, Belgium. Cord and peripheral blood mononuclear cells were isolated using standard Ficoll-Hypaque (Amersham Pharmacia Biotech, Piscataway, NJ) gradients centrifugation. Blood specimens were collected under protocols approved by the Institutional Review Boards of the above mentioned Institutions.

2.1.2. FACS analysis and sorting

Cell surface analysis and sorting were performed using a combination of a panel of surface markers: PercP or PercP Cy5.5 conjugated mouse anti-human CD4 (Becton Dickinson, Franklin, NJ), APC-conjugated mouse anti-human CD25 (BD PharMingen, San Diego, CA), PE-conjugated mouse anti-human CD62L or PE-conjugated mouse anti-human CD71 (Becton Dickinson, Franklin, NJ), FITC or PE-conjugated mouse anti-human CD45RO (BD

PharMingen, San Diego, CA) and FITC Annexin-V (Becton Dickinson, Franklin, NJ). For cell-sorting experiments $CD4^+$-$CD25^+CD62L^+CD45RO^-$, $CD4^+CD25^+CD62L^+CD45RO^+$,$CD4^+CD25^-CD62L^+CD45RO^-$ and $CD4^+CD25^-CD62L^+$-$CD45RO^+$ cell populations were isolated from the peripheral blood. The grade of cell purity in all the sorting experiments was more than 97%. All flow cytometric analyses were performed on a FACS Calibur and cell sorting on a FACS Aria (Becton Dickinson Systems, Franklin, NJ). For intracellular FOXP3 analysis, cell preparations were fixed and permeabilized with fixation/permeabilization buffers (eBioscience) after staining of cell surface markers and stained with FITC-conjugated rat antihuman FOXP3 (eBioscience).

Regulatory T cells have been sorted and purified from peripheral and cord blood based on a $CD4^+CD25^{high}$-$CD62L^+$ gate. In order to analyze the purity of naturally occurring T_{regs}, the above population has been stained for Foxp3. It is clear from Fig. 1 that the cells sorted with this method are in majority Foxp3 positive. $CD4^+$-$CD25^-CD62L^+$ cells have been sorted and stained in the same way. The majority of all $CD25^-$ cells are Foxp3 negative. Naturally occurring T_{regs} express CD25 constitutively and contrary to recently activated $CD25^-$ T cells, they do not downregulate this receptor. It is not excluded that the above sorting from peripheral blood involves some adaptive T_{regs} which are also included in the mathematical model presented hereafter.

2.1.3. Suppression assay

Sorted purified $CD4^+CD25^-$ T cells have been stimulated *in vitro* with anti-CD3 and anti-CD28 antibodies for 3 days alone (positive control) or in the presence of sorted purified $CD4^+CD25^+CD62L^+CD45RO^+$ T cells to test the suppressive function of the latter on the proliferation capacity of the former population. $CD4^+CD25^+$-$CD62L^+CD45RO^+$ T cells have been added directly in the same well or in a transwell to test if their suppressive function needs cell-to-cell contact or is mediated by cytokines. $CD4^+CD25^+CD62L^+CD45RO^+$ T cells were able to highly suppress (96%) the proliferation of $CD4^+$-$CD25^{neg}$ T cells when co-cultured in the same well, but lost all suppressive activity once cultured in a transwell (Fig. 2).

2.1.4. Proliferation, activation and differentiation experiments

In order to assess the proliferation capacity, peripheral blood sorted cell populations ($CD4^+CD25^+CD62L^+$–$CD45RO^-$, $CD4^+$

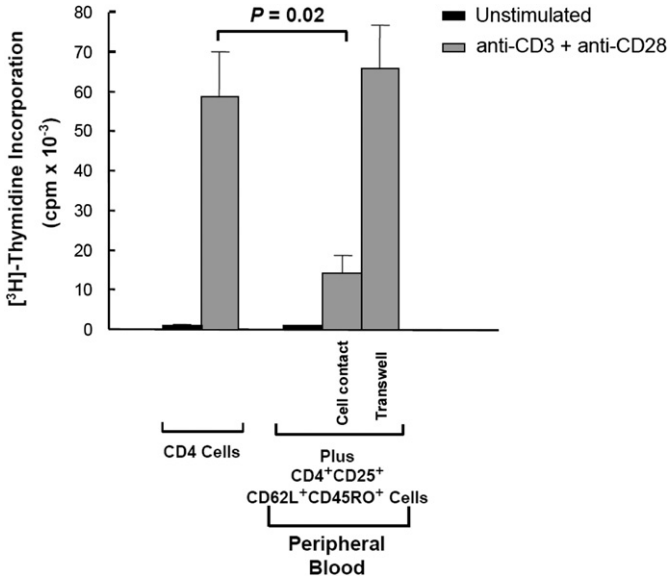

Fig. 2. Cell-to-cell contact is needed by the $CD4^+CD25^+CD62L^+CD45RO^+$ T cells to exert their suppressive function, while cytokines do not seem to play any role.

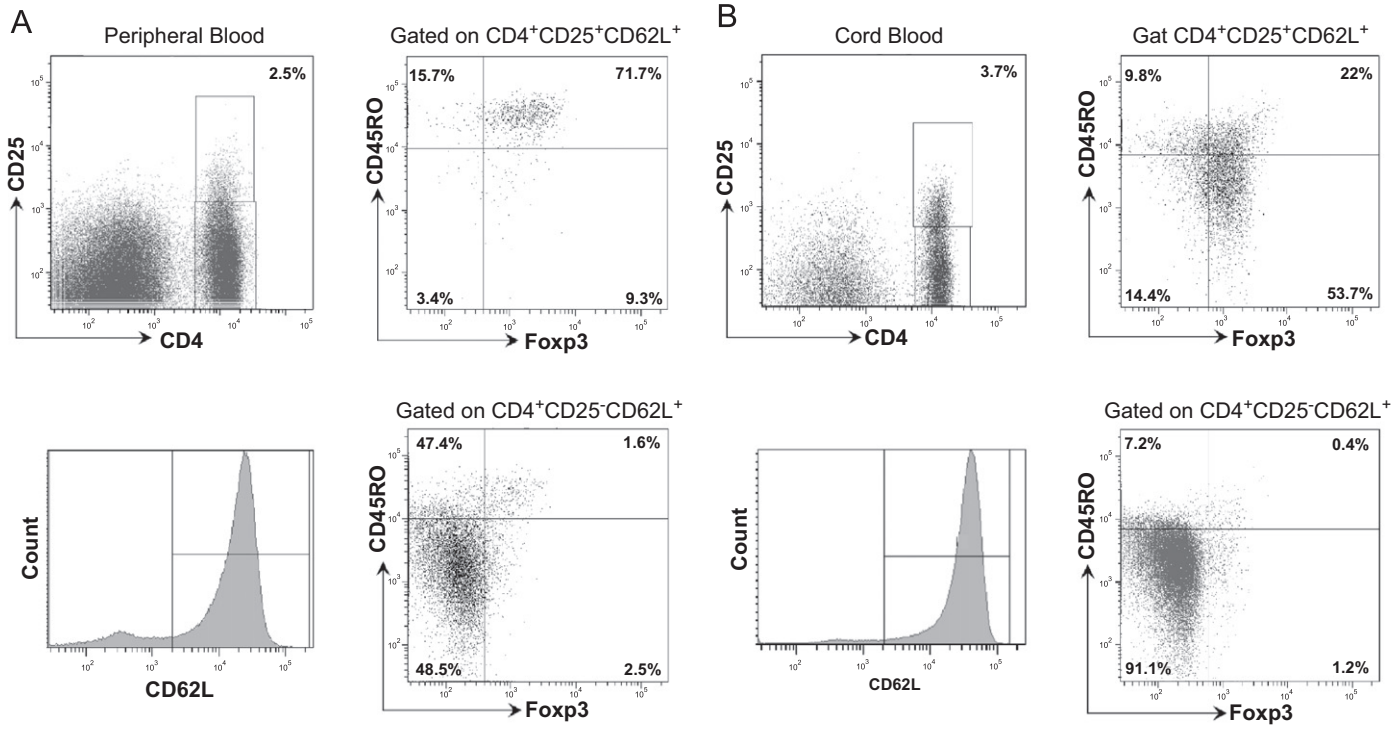

Fig. 1. Isolation and characterization of human $CD4^+CD25^+$ T_{regs} from peripheral and cord blood. (A) Representative flow cytometry profiles of one peripheral blood sample (1 out of 120). (B) Representative flow cytometry profiles of one cord blood sample (1 out of 7). Regulatory T cells have been sorted and purified from peripheral and cord blood based on the gate on $CD4^+CD25^{high}CD62L^+$ cells; the gate for non-regulatory T cells was on $CD4^+CD25^{neg}CD62L^+$ cells. In both peripheral and cord blood, the majority of $CD4^+CD25^+$ cells are $Foxp3^+$ and the majority of $CD4^+CD25^-$ cells are $Foxp3^-$.

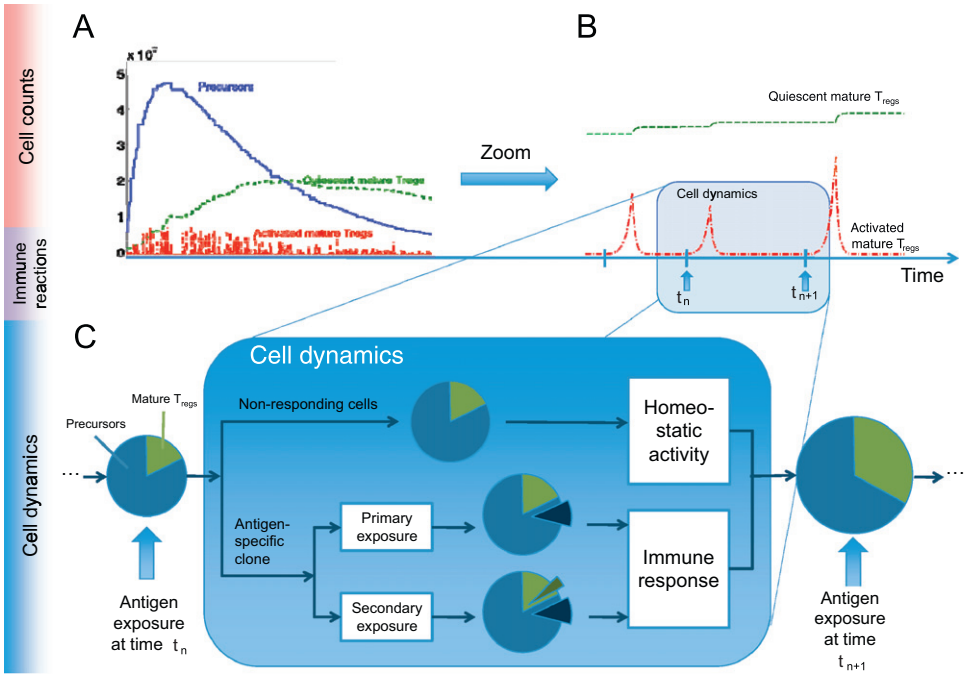

Fig. 3. A sketch of the different components of the mathematical model. (A) The output of our mathematical model are cell counts as function of time. We are considering three cell types, namely $CD4^+CD25^+CD45RO^-$ precursor T_{regs} and $CD4^+CD25^+CD45RO^+$quiescent or activated mature T_{regs}. (B) The model is composed of a stochastic process generating the events corresponding to successful encounters with antigen-presenting cells leading to (auto-)immune responses. These responses are characterized by a transient increase in the activated mature T_{regs} population. (C) The dynamics of cells between two events of the stochastic process are described using ordinary differential equations. These equations take into account all events that affect the cell population size. A detailed description of each component of the cell dynamics can be found in the Generic Model section.

$CD25^+CD62L^+CD45RO^+$, $CD4^+CD25^-$–$CD62L^+CD45RO^-$ and $CD4^+CD25^-CD62L^+CD45RO^+$) were plated at 5×10^3 cells per well in 96 U-bottomed plates in RPMI 1640 plus 10% FBS in the presence of 5×10^4 irradiated (4000 rad) syngeneic peripheral blood mononuclear cells. Cells were cultured in the presence of soluble anti-CD3 (OKT3) plus soluble anti-CD28 (BD Pharmingen, San Diego, CA) with or without IL-2. The proliferation kinetic was followed by FACS over 15 days and by [3H]-Thymidine incorporation in correspondence of proliferative peaks. The activation and differentiation were monitored during 15 days by the expression of activation markers such as CD25 and CD71 (Transferrin Receptor) and the marker of mature cells CD45RO. Cell death by apoptosis was measured in parallel for each population by the expression of Annexin-V.

2.1.5. *Extrapolation of a mathematical model from empirical observations*

Prior to formulating a mathematical model, we studied the proliferation kinetics of three populations ($CD4^+CD25^+CD62L^+CD45RO^-$, $CD4^+CD25^+CD62L^+CD45RO^+$, and $CD4^+CD25^-CD62L^+CD45RO^-$ cells) that may be involved in the maintenance of a constant pool of regulatory T cells. The assay was performed several times using sorted cells from different subjects in order to extrapolate some parameter values for the model, free from the individual vices. Each of the sorted cell populations was cultivated in the presence of a polyclonal stimulus in order to stimulate all the clones contained in a population. All the experiments were designed in such a way that IL-2 is added at the beginning of the culture and every two days, because of the limited proliferation capacity of mature T_{regs}. In fact, these cells did not show any appreciable proliferation in other parallel experiments driven in the absence of IL-2. Each experiment lasted 15 days to permit the estimation of parameter values such as the duration of the proliferation phase, the amount of cells produced, the number of cells that were activated ($CD71^+$), differentiated and acquired a mature phenotype ($CD45RO^+$), the cell death ($Annexin^+$ cells) and the number of surviving cells. We then studied retrospectively the distribution of the above populations in the peripheral blood of 120 healthy individuals, seven cord blood samples and two thymuses, obtained from two children of 1 and 3 years old, who underwent cardiac surgery. In this way, we obtained the distribution of the above populations as a function of age.

2.2. *Mathematical model*

In order to model the biological hypotheses concerning the origins and the proliferation capacity of T_{regs}, we consider several scenarios of a generic mathematical model. The scenarios are the result of imposing constraints on model parameters such as the input, proliferation and death rates of precursor and mature T_{regs} in the generic model.

We use several mathematical tools in order to describe in a robust way T_{regs} lifelong kinetics. Changes in the populations' sizes due to immune reactions and homeostatic activity are described by ordinary differential equations (ODEs). Events corresponding to encounters with antigen-presenting cells, which lead to (auto-)immune responses, are generated according to a stochastic process. A sketch of the entire system with all its components can be seen in Fig. 3. For a quick reference, Table 1 summarizes all the assumptions of our model. In the following section, we describe in detail the generic model, the model scenarios, the parameter fitting and the model evaluation procedure.

2.2.1. *Generic model*

The generic model describes the lifelong dynamics of T_{regs}. We call it generic because it is taking into account all possible events that may affect T_{regs} population size and because it is a generalization out of which we define the model scenarios that describe

Table 1
Summary of all model assumptions.

Biological process		Assumptions
(Auto-)Immune reactions process	1.	Major immune reactions modeled as a stochastic process with one (constant) parameter
	2.	Minor immune reactions triggered by antigens sampled in the mucosa-associated lymphoid tissues included in the homeostasis activity
	3.	Capacity to present self-peptides is not altered with age in healthy individuals
	4.	During the fixed phase of an immune reaction, no other reactions are allowed
Immune responses	5.	Two-phase immune response: a first phase of fixed length and a second phase of random length
	6.	Exponential expansion/contraction of cells following immunogen stimulation
	7.	10% of the expanded population of activated T_{regs} becomes long-lived mature T_{regs}
Homeostatic activity	8.	Unique source of precursors: thymus
	9.	Four possible sources of mature T_{regs}: thymus, differentiation of precursors, phenotype switching of effector $CD4^+CD25^-$ T cells, and homeostatic proliferation
	10.	Time-dependent thymic involution (exponential decline)
	11.	Constant rate of generation of T_{regs} from rapidly proliferating $CD4^+CD25^-$ effector T cells under certain conditions
Antigen specificity	12.	The size of the responding clone is chosen randomly (uniform distribution)
Primary/ secondary infections	13.	The probability of primary infections is declining with age and is such that children experience a majority of primary infections and adults, a majority of secondary infections

the studied biological hypotheses. The generic model is composed of two parts: a deterministic part describing cell dynamics during immune responses and homeostasis, and a stochastic part generating all infection events occurring in a human lifetime.

(*Auto-*)*Immune reactions process*: In order to study the dynamics of regulatory T cells over the entire lifetime of a human, responses to self- and foreign-antigens are included in our model. We consider two types of immune reactions: the minor ones, occurring frequently and triggered by self- or dietary antigens, and the major ones, occurring rather seldom, mainly provoked by foreign antigens and having a great impact on the T_{regs} pool. Minor immune reactions triggered by antigens sampled in the mucosa-associated lymphoid tissues are taken into account in the pool-size control dynamics described in the next section. Major immune reactions are triggered by successful interactions with antigen-presenting cells, in which a cytokine environment allowing T_{regs} activation and (possibly) proliferation is present (Carneiro et al., 2007). As we found no information about the frequencies and time-distribution of such immune reactions *in vivo*, we model this phenomena with a stochastic process having a constant rate. Thus, we assume the length of time-intervals between two infections to be random, having a shifted exponential distribution with mean $\lambda+\delta$, where δ is the minimal duration of an immune response. We make the simplifying assumption that during the first phase of an immune response (of length δ), no other infections are occurring and that the capacity to present self-peptides is not altered with time in healthy individuals. We call $\{\tau_n\}_{n\in\mathbb{N}}$ the stochastic process of infection times. The dynamics of cells between the events of the stochastic process are described in what follows.

Cell dynamics: Based on the expression of the surface protein CD45RO, one can sort two subpopulations of T_{regs}: $CD4^+CD25^+$ $FoxP3^+CD62L^+CD45RO^-$ precursor and $CD4^+CD25^+$-$FoxP3^+$ $CD62L^+CD45RO^+$ mature T_{regs}. For the sake of the mathematical model, we consider a third population that we call *activated mature* T_{regs} and that has the same surface receptors as the *quiescent mature* T_{regs}. Activated mature T_{regs} are composed of both precursors that experience peripheral antigens for the first time (they can be also activated precursors that have just acquired the mature phenotype), and mature T_{regs} that are recruited into a secondary immune response. Thus, the mathematical model has three compartments: P, the precursor T_{regs}, Q, the quiescent mature T_{regs}, and R, the activated mature T_{regs}. Let $Y=(P,Q,R)'$.

(a) *Immune responses*: *In vitro* experiments show that following acute antigenic stimulation, precursor T_{regs} activate and up-regulate the memory-type CD45RO receptor, as they loose their naive phenotype CD45RA receptor (Valmori et al., 2005; Fritzsching et al., 2006). In the meanwhile, they differentiate into mature T_{regs} able to exert their suppressive function. Once the antigenic stimulation is lost, a small proportion of all activated T_{regs} becomes long-lived mature cells, and the others die by apoptosis, similarly to other lymphocytes. As we are not modeling the dynamics of other cell types and of pathogens, we apply the two-phase immune response model used to describe $CD4^+CD25^-$ and $CD8^+$ cell dynamics (De Boer et al., 2001, 2003; Althaus et al., 2007; Fouchet and Regoes, 2008). We call τ_n the beginning of the nth immune response to a foreign antigen ($n\in\mathbb{N}$) and $\tau_n+\delta$ the time at which the expansion phase ends. We assume that the effect of antigen on cells has a fixed duration δ, after which cells stop their intense proliferation phase (Phase 1) and start dying by activation-induced cell death (Phase 2).

During Phase 1, precursor T_{regs} may divide, die, or convert into mature effector cells at rate b. Quiescent mature T_{regs} activate at rate f cells per day. Effector mature T_{regs} may also proliferate and die. As the first phase is an expansion phase, we only consider a net population expansion rate, which should be interpreted as the cumulative effect of proliferation and death in the population of precursors (resp. activated mature T_{regs}). Thus, for parameter identification issues, we consider only one rate, called $a_P>0$ (resp. $a_R>0$), which is the net population expansion rate. The following differential equations express the dynamics of the expansion phase:

$$\begin{aligned}\dot{P}&=(a_P-b)P\\ \dot{Q}&=-fQ\\ \dot{R}&=bP+fQ+a_RR\end{aligned}\qquad(1)$$

During Phase 2, precursor T_{regs} die at rate d_P per day. Activated mature T_{regs} die at rate d_R and convert to long-lived mature cells at rate c per day. The long-lived mature quiescent T_{regs} have a slight decrease in their population size expressed by death rate d_Q. The differential equations corresponding to the contraction phase are the following:

$$\begin{aligned}\dot{P}&=-d_PP\\ \dot{Q}&=-d_QQ+cR\\ \dot{R}&=-(c+d_R)R\end{aligned}\qquad(2)$$

(b) *Homeostatic activity*: The biological processes included in the homeostatic activity are (1) the proliferation and death of cells for regulation of the population size, (2) the death of cells because of their limited lifespan and (3) the input of newly produced cells

from the thymus or from another external source. We hypothesize two types of basal proliferation and death: a constant and density-dependent one. We call d' the constant death rate, accounting for the limited lifespan of cells. We assume that a slow and steady cell division occurs at rate a'. Nevertheless, these constant renewal and death rates cannot account for self-regulation of the cell population size. In a homeostatic situation, cell numbers are regulated by competition for limited resources, such as cytokines. This regulation can be achieved in three ways: density-dependent proliferation, density-dependent death or both. The exact way in which regulatory T cells perform their homeostatic regulation is currently unknown. It is however known that the *in vivo* homeostatic proliferation of murine natural T_{regs} is not impaired by their anergic state (Gavin et al., 2002) and that this proliferation is involved in a feedback regulatory loop between dendritic cells and T_{regs} (Darrasse-Jeze et al., 2009). Because the homeostatic activity is an important issue to the study of the lifelong dynamics of cells *in vivo*, we consider all possible mechanisms that may have an effect on the model's outcome. Thus, we assume that homeostasis of precursors is achieved through density-dependent death at rate φ_P. For mature T_{regs}, we consider both a density-dependent death at rate φ_Q and a density-dependent Michaelis–Menten type proliferation at rate α, appropriate to make up for lymphopenic situations. Recent thymic emigrants enter both precursor and mature T_{regs} populations at a time-dependent rate $g(t) = g_P(t) + g_Q(t)$. The constant term s_Q, added to the quiescent mature T_{regs} population, represents the constant generation of regulatory T cells from rapidly proliferating $CD4^+CD25^-$ effector T cells under certain conditions (Vukmanovic-Stejic et al., 2006; Akbar et al., 2007). Remark that we only add this term to the quiescent mature T_{regs} population, because we assume that the unique source of precursor $CD4^+CD25^+CD45RO^-$ T cells is the thymus. In addition, cells that are derived from rapidly proliferating $CD4^+CD25^-$ cells are antigen-experienced and thus have probably acquired the memory phenotype CD45RO before converting to $FoxP3^+$ regulatory cells. The differential equations describing the homeostatic activity are the following:

$$\dot{P} = g_P(t) + (a'_P - d'_P)P - \varphi_P P^2$$

$$\dot{Q} = \underbrace{g_Q(t) + s_Q}_{\substack{\text{External}\\ \text{contribution}}} + \underbrace{(a'_Q - d'_Q)\,Q}_{\substack{\text{Density-independent}\\ \text{regulation}}} + \underbrace{\left(\frac{\alpha}{1+Q/Q_M} - \varphi_Q Q\right) Q}_{\substack{\text{Density-dependent}\\ \text{regulation}}}$$

$$\dot{R} = 0, \tag{3}$$

where Q_M is the size of the mature T_{regs} population for which the homeostatic renewal of cells is half of the maximal rate α. Let $h_P = a'_P - d'_P$ and $h_Q = a'_Q - d'_Q$ be the cumulative effects of the constant renewal/death rates, $h_P \in \mathbb{R}$ and $h_Q \in \mathbb{R}$. Whenever negative, we will refer to these parameters as lifespan of precursors and mature T_{regs}. The thymic involution is represented as a decreasing exponential function of rate v (Steinmann et al., 1985; Marušić et al., 1998; Dutilh and De Boer, 2003):

$$g_P(t) = \sigma_P \exp(-vt)$$

$$g_Q(t) = \sigma_Q \exp(-vt)$$

where $\sigma_P = \sigma_0 * \%CD25_{thymus} * p_{thymus}$, $\sigma_Q = \sigma_0 * \%CD25_{thymus} * (1-p_{thymus})$, $\%CD25_{thymus}$ is the percentage of $CD25^+$ cells inside thymic $CD4^+$ T cells, p_{thymus} is the percentage of precursors inside $CD25^+$ cells that are output from the thymus, and σ_0 is the estimated thymic output of $CD4^+$ cells in a newborn.

(c) *Antigen specificity*: Antigen specificity is implemented in the following way. Eqs. (1) and (2) are applied to a proportion π_n of the total number of cells, those representing the antigen-specific clone responding to the antigen that caused the immune reaction at time τ_n. We call this population $Y_{clone}(\tau_n)$. The other $1-\pi_n$ proportion of cells do not participate in the nth immune reaction and execute their homeostatic activity (Eq. (3)).

(d) *Primary/secondary infections*: We take into account the difference between primary and secondary infections: when some antigen is encountered for the first time, no memory cells exist, but if the exposure is secondary, the organism already has memory cells associated to it at the time of exposure τ_n. We call $q(t)$ the probability that an infection at time t is primary and does not involve mature T_{regs}. Thus, with probability $q(\tau_n)$, the responding clone at time τ_n is set to $Y_{clone}(\tau_n) = \pi_n(P(\tau_n),0,0)'$. Otherwise, with probability $1-q(\tau_n)$, the responding clone is set to $Y_{clone}(\tau_n) = \pi_n(P(\tau_n),Q(\tau_n),0)'$. Intuitively, the unexperienced immune system of young individuals is confronted with more primary infections than those of adults. We therefore define the following sigmoid function that describes phenomenologically the time-dependence of parameter q:

$$q(t) = \frac{K_1 - K_2}{1 + \exp(\omega(t - t_h))} + K_2 \tag{4}$$

where K_1 is the (approximate) proportion of primary infections at birth, K_2 is the limit proportion of primary infections at adulthood, ω is the maximum decline rate and t_h is the age at which the proportion of primary infections is $q(t_h) = (K_1 + K_2)/2$. Note that contrary to $CD4^+CD25^-$ memory T cells, mature T_{regs} require additional conditions for their activation at the time of a secondary antigen exposure. Because these cells are non-proliferating and do not produce the growth factor IL-2 themselves, they need optimal stimulation conditions and a high concentration of IL-2 in order to initiate a response (Hombach et al., 2007). All this is taken into account in the above definition of $q(t)$.

2.2.2. Model scenarios

The model scenarios are obtained from the generic model by applying a set of constraints to the following parameters: $g_Q(t), s_Q, \varphi_Q, \alpha, a_P, a_R$ and d_P. From the homeostasis dynamics of the generic model, we define three *homeostasis scenarios*:

(i) No homeostatic regulation of mature T_{regs}: Due to their anergic state, the only observed phenomena is the slow and steady density-independent proliferation and death ($g_Q(t) = s_Q = \varphi_Q = \alpha = 0$).

(ii) Homeostatic regulation of mature T_{regs}: In addition to the constant proliferation and death rates, we allow for density-dependent regulation mechanisms of mature T_{regs}. As we search for the minimal model that explains the data, we consider two mutually exclusive sub-settings:
   (a) density-dependent death of mature T_{regs} ($\varphi_Q > 0, \alpha = 0$);
   (b) density-dependent proliferation of mature T_{regs} ($\varphi_Q = 0, \alpha > 0$).

(iii) External input: we consider two external contributions to the mature T_{regs} population ($\alpha = 0$):
   (a) thymic output of mature T_{regs} (Vanhecke et al., 1995) ($g_Q(t) > 0$);
   (b) peripheral differentiation of $CD4^+CD25^-$ non-regulatory cells into their regulatory counterpart (Vukmanovic-Stejic et al., 2006) ($s_Q > 0$).

From the cell dynamics in response to self- and foreign antigens, we define four *proliferation scenarios* accounting for different proliferation capacities of T_{regs}:

(1) Both precursor and activated-mature T_{regs} proliferate and die in response to an antigen stimulus.

(2) Neither precursor nor mature T_{regs} proliferate, but precursors are very resistant to apoptosis, so they do not die during an immune response.
(3) Precursors proliferate in response to antigen, but as soon as they differentiate into $CD45RO^+$ mature T_{regs}, they stop proliferating and die extensively because of the high levels of expression of the CD95 receptor (Fritzsching et al., 2006) and because of the downregulation of the antiapoptotic protein Bcl-2 (Yamaguchi et al., 2007).
(4) Precursors do not proliferate when they are $CD45RO^-$, but the proliferation starts while they acquire the mature profile.

Tables 2 and 3 summarize the above settings. We construct a *model scenario* by choosing one homeostasis and one proliferation scenario, thus obtaining 20 model scenarios, referred from now on as scenario 1(i), 2(i), …, 4(i), 1(ii)a, …, 4(ii)b, 1(iii)a, …, 4(iii)b.

2.2.3. The model at a glance: typical model trajectories

In order to gain some insight into the model dynamics, we present in this section an example of execution of our model. Fig. 4 shows the number of precursors (solid line) and mature T_{regs} (resting: dashed line and activated: dash-dotted line) as a function of time in human peripheral's blood. The zoomed sections allow for a closer look at the activated T_{regs} population that is mainly present during major immune reactions, which are events of the stochastic process.

Fig. 4A depicts a typical trajectory for scenario 1(i) where the ratio between precursors and mature T_{regs} is inverted in the early years of adulthood, whereas Fig. 4B shows a typical trajectory for scenario 2(i) where the ratio inversion is not observed. All model scenarios will be evaluated based on their capacity to reproduce this ratio inversion and on the capacity to reproduce the total amount of T_{regs} suggested by the data. Note that because the thymus produces thymocytes with a constant proportion of each subtype of T_{regs}, there are four means of achieving a precursor/mature T_{regs} ratio inversion: (1) a difference in lifespans of precursors and mature T_{regs}; (2) a difference in the homeostatic proliferation rates of precursors and mature T_{regs}; (3) the slow accumulation of mature T_{regs} following an antigen stimulation; (4) an external source of mature T_{regs}. The first mean is present in all model scenarios and it acts in combination with the other three means. Thus in each model scenario, we observe a combination of the above means, and this combination can be sufficient or not to achieve the ratio inversion. For example, in Fig. 4 where there is no homeostatic regulation, the lifespan of precursors is larger than the lifespan of mature T_{regs} ($|h_P| > |h_Q|$), but this lifespan difference is not sufficient to achieve the ratio inversion. Here, the slow accumulation of mature T_{regs}, present in scenario 1(i) and not in scenario 2(i), is needed.

2.2.4. Parameters

In order to cope with the large number of parameters and to decrease the effect of single values on the dynamics of the model, we split the parameters into two groups: G_1, parameters for which some *a priori* information is found, and G_2, unknown parameters that must be fitted to the data. The probability distribution of parameters of group G_1 is defined in the following way: we find in the literature either a parameter together with a confidence interval accounting for the uncertainty of the estimation or a finite range without any preferred value specified. In the former case, we use a Gaussian distribution with mean and variance given by the confidence interval. In the latter case, we use a uniform distribution over the range. Table S0 of the Supplementary Material summarizes all parameter distributions.

Our *in vitro* assays have shown that the expansion rate a_P of T_{regs} precursors is similar to the one of $CD4^+CD25^-$ naive T cells and that the expansion rate a_Q of activated mature T_{regs} is 1.4–2 times lower than the expansion rate of precursors. To our knowledge, the *in vivo* expansion rate of precursors (or even of $CD4^+CD25^-$ naive T cells) in humans has not yet been measured. The *in vivo* T cell responses in mice have been quantified in De Boer et al. (2003) which gives a first idea about the order of magnitude of parameters such as the proliferation and death rates of $CD4^+$ T cells, as well as the duration of a T cell response. For a_P, we find in De Boer et al. (2003) values in the range 1–1.7 per day, so we are sampling from an uniform distribution between 1 and

Table 2
Definition of the homeostasis scenarios.

	Homeostasis scenarios	Parameter setting
(i)	No homeostasis	$g_Q(t) = 0$, $s_Q = 0$, $\varphi_Q = 0$, $\alpha = 0$
(ii)	Homeostatic regulation	
	(a) Density-dependent death	$g_Q(t) = 0$, $s_Q = 0$, $\varphi_Q > 0$, $\alpha = 0$
	(b) Density-dependent proliferation	$g_Q(t) = 0$, $s_Q = 0$, $\varphi_Q = 0$, $\alpha > 0$
(iii)	External input	
	(a) From thymus	$g_Q(t) > 0$, $s_Q = 0$, $\varphi_Q = 0$, $\alpha = 0$
	(b) Peripheral differentiation of $CD4^+CD25^-$ T cells	$g_Q(t) = 0$, $s_Q > 0$, $\varphi_Q = 0$, $\alpha = 0$

Parameter meanings: $g_Q(t)$, time-dependent input of recent thymic emigrants into the peripheral mature T_{regs} population; s_Q, constant input of regulatory T cells from rapidly proliferating $CD4^+CD25^+$ effector T cells, φ_Q and α are the density-dependent death and proliferation rates.

Table 3
Definition of the four proliferation scenarios.

Proliferation scenarios	Proliferation capacity of …		Parameter setting
	Precursors	Mature T_{regs}	
1	Proliferate	Proliferate	$a_P > 0$, $a_R > 0$, $d_P > 0$
2	Do not proliferate	Do not proliferate	$a_P = 0$, $a_R = 0$, $d_P = 0$
3	Proliferate	Do not proliferate	$a_P > 0$, $a_R = 0$, $d_P > 0$
4	Do not proliferate	Proliferate	$a_P = 0$, $a_R > 0$, $d_P = 0$

Parameter meanings: a_P, antigen-induced proliferation rate of precursors; a_R, antigen-induced proliferation rate of mature T_{regs}; d_1, antigen-induced death rate of precursors.

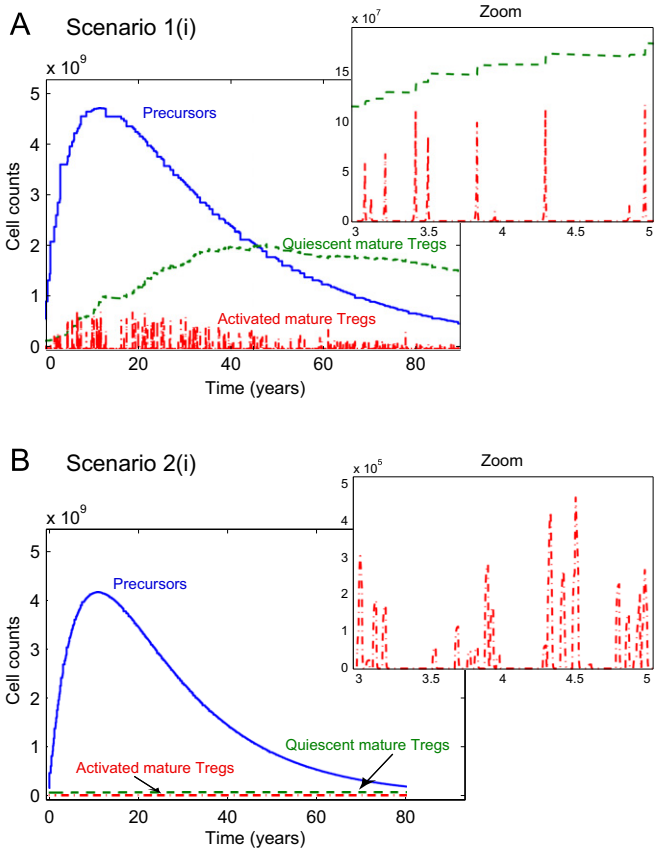

Fig. 4. Typical model trajectories for scenarios 1(i) and 2(i). The solid line represents the evolution of precursors, the dashed one the dynamics of quiescent mature T_{regs}, and the dash-dotted line represents the activated mature T_{regs}. Each spike of the activated mature T_{regs} corresponds to a major immune reaction (an event of the stochastic process). The ratio inversion observed in (A) is an example of slow accumulation of mature T_{regs} following an antigen stimulation. Parameter values: average values of the distributions of Table 4 with the following values for the fitted parameters: $h_P = -5\times10^{-4}$, $h_Q = -5\times10^{-5}$, $\lambda = 130$ for scenario 1(i), and $h_P = -5\times10^{-4}$, $h_Q = 0$, $\lambda = 30$ for scenario 2(i).

1.7 per day ($a_P \sim \mathcal{U}(1,1.7)$). We set $a_R = a_P/K$, where K takes two different values, 1.4 and 5, the latter being an extreme value representing the case where mature T_{regs} have a very limited proliferating capacity compared to precursors. The value of the differentiation rate b of precursors into mature T_{regs} defines two settings: in the first, $b \sim \mathcal{U}(1,10)$ (Burroughs et al., 2006) and in the second, we apply the constraint $b \le a_P$, thus $b \sim \mathcal{U}(0.5,1)$. We will see that these settings give slightly different results. The activation rate of quiescent mature T_{regs} is set to half of the differentiation rate of precursors, i.e., $f = b/2$, because mature T_{regs} are anergic and thus slow to activate. The duration δ_n of the expansion phase is drawn from a Gaussian distribution $\mathcal{N}(7.65,0.72)$ (*in vitro* assay and De Boer et al., 2003). Both death rates d_P and d_R are considered as uniform $\mathcal{U}(1,2)$ because they should have similar or higher values to the proliferation rates for system stability issues. It is known that $\sim 5-10\%$ of all effector cells become long-lived memory cells. Thus, we set $c = d_R/9$, which corresponds to 10% of the maximum value of the effector response. The death rate d_Q is distributed according to $\mathcal{N}(0.0013,0.0002)$ (De Boer et al., 2003).

The thymic input is calculated as follows. For the value of the total number of $CD4^+$ T cells output from the thymus of a newborn (σ_0) and for the thymic involution rate (ν), we found the following parameter settings in literature: $\sigma_0 = 1.98\times10^8$ cells per day and $\nu = 0.024$ per year (Marušić et al., 1998; Steinmann et al., 1985); $\sigma_0 = 4.48\times10^8$ cells per day and $\nu = 0.05$ per year (Dutilh and De Boer, 2003; Clark et al., 1999). We therefore use an uniform distribution $\mathcal{U}(1\times10^8, 5\times10^8)$ for σ_0 and $\mathcal{U}(0.01,0.06)$ for ν to include the above settings in our simulations. The percentage of $CD25^+$ cells among all $CD4^+$ thymocytes ($\%CD25_{thymus}$) was measured to be 1.3% in young children (unpublished data).

The proportion π_n, $n \in \mathbb{N}$, of cells that respond to a particular antigen is drawn uniformly between 10^{-7} and 10^{-4} cells. To estimate the total number of T cells in human's peripheral blood as a function of age, $T(t)$, we use the fact that the mean blood volume of a healthy 70 kg individual is 5 l (Feldschuh and Enson, 1977) and it contains about 10^{11} T cells (Clark et al., 1999). We then use a function that maps age to the mean weight of individuals (WHO, 2009; CDC, 1988–1994).

The constant and density-dependent homeostatic proliferation and death rates (h_P, h_Q, φ_P, φ_Q, α, Q_M), as well as the infections occurrence rate (λ) and the external input from the thymus (p_{thymus}) or from $CD25^-$ conversion (s), are fitted to the data. The time-unit of the model is 1 day.

2.2.5. *Model evaluation procedure and parameter fitting*

The model assessment procedure consists of the following steps: first, we consider the mean model dynamics and we fit the unknown parameters to the biological data using a least-squares procedure (implemented in Matlab). The mean model is derived from the stochastic one by fixing the parameters of group G_1 to the mean value of their *a priori* distribution and by averaging over the remaining random quantities. The latter are Y_{clone}, the size of the responding clone, and $\Delta_n = \tau_{n+1} - \tau_n$, the time-interval between two consecutive immune reactions. Based on this fit, we can reject some model scenarios. However, this result may depend on the mean values of the *a priori* distributions. In order to eliminate this possibility, we fit the stochastic model (in which parameters of group G_1 are random variables) using a Bayesian approach. This fit consists in maximizing the likelihood function, a measure of how good is the model in explaining the data. It is the probability that, given the best-fit parameters and the *a priori* distributions, the data are a realization of a particular model scenario. The higher this probability, the closer the model is to the data. The likelihood of a model scenario is computed as follows.

Consequently to the fact that the parameters of group G_1 are defined as random variables, $\{P(t)\}_{t\in\mathbb{R}}$, $\{Q(t)\}_{t\in\mathbb{R}}$ and $\{R(t)\}_{t\in\mathbb{R}}$ are stochastic processes. In order to fit each model scenario to the biological data, we transform the above processes in the format of the data, i.e., in terms of the ratio precursor/mature T_{regs} and of the percentage of $CD4^+CD25^+$ cells inside all T cells, in logarithmic scale. Thus, we consider two other stochastic processes, namely $\{U(t)\}_{t\in\mathbb{R}}$ and $\{V(t)\}_{t\in\mathbb{R}}$, given by

$$U(t) =: \log\left(\frac{P(t)}{Q(t)+R(t)}\right)$$

$$V(t) =: \log\left(\frac{P(t)+Q(t)+R(t)}{T(t)}\right),$$

where $T(t)$ is the total number of T cells at time t.

Let $g_{UV}(u,v;\,t)$ be the joint density of U and V. Because it is difficult to compute $g_{UV}(u,v;\,t)$ analytically, we estimate it using Monte Carlo simulation, as follows. The model is executed M times for a time horizon of 85 years with parameters drawn according to the distributions of Table S0 of the online Supplementary Material. At each time, the density of trajectories in the space of U and V is estimated using a bivariate histogram. Call $\hat{g}^{(s)}_{UV}(u,v;t)$ the estimated density of model scenario s at time t. Using the M model replicates, we construct a confidence interval for the bivariate histogram (Davison, 2003). We then consider the relative size of the confidence interval of each bin. If the latter is greater than 10% for some bin, the number of replicates M is

increased. The density estimation is considered satisfactory if the relative size of the confidence interval of all bins is smaller than 10%. In the case of our model scenarios, M is taking values between 100 000 (in most cases) and 500 000.

Each model scenario s is fitted to the data by maximizing the log-likelihood function defined as

$$\ell_s(\theta) = \sum_{i=1}^{N} \log(\hat{g}^{(s)}_{UV}(u_i, v_i; \theta | t_i)), \quad \theta \in \Theta_s,$$

where N is the number of data points (N=126) and $\hat{g}^{(s)}_{UV}(u_i, v_i; \theta | t_i)$ is regarded as a function of θ for (u_i, v_i) and t_i fixed. The parameter space Θ_s is defined by the values that can take the free parameters $\theta = (h_P, h_Q, \lambda, \varphi_P, \varphi_Q, Q_M, \alpha, p_{\text{thymus}}, s)$.

The log-likelihood is also used for objectively comparing the different model scenarios by performing a likelihood ratio test (F-test) for nested models that formally rejects the scenarios that are not compatible with the data. Two models are nested if the parameter space of one of them is a subset of the parameter space of the other. Proliferation scenarios 2, 3 and 4 (null hypothesis) are subsets of scenario 1 and homeostasis scenario (i) (null hypothesis) is a subset of all other homeostasis scenarios. The null hypothesis is rejected if the p-value of the test is < 0.01.

3. Results

3.1. Properties of T_{regs} dynamics

The immunological data are presented in Fig. 5, in which are plotted A: the percentage of $CD4^+CD25^+$ cells inside all T cells, B: the ratio $CD4^+CD25^+CD45RO^-$ precursor/$CD4^+CD25^+CD45RO^+$ mature T_{regs} as a function of age and C: the proportions of precursor and mature T_{regs} inside the $CD4^+CD25^+$ compartment. A direct analysis of the above data sets allows the identification of two properties.

3.1.1. Homeostasis is maintained over both $CD4^+CD25^+CD45RO^-$ precursor and $CD4^+CD25^+CD45RO^+$ mature T_{regs} populations:

Consider the data of Fig. 5(A) corresponding to adulthood, i.e., ages 19–81. In order to see whether the population of $CD4^+CD25^+$ cells is in equilibrium, we need to know if there is a significant trend in these data. The best-fit of a linear regression model results in a 95% confidence interval of the slope that contains zero (slope $= -0.0034$, 95% confidence interval: $[-0.0071, 0.0003]$). Thus the trend is not significant, suggesting that the population of $CD4^+CD25^+$ T_{regs} is in equilibrium and that there is a common homeostatic mechanism to both $CD4^+CD25^+CD45RO^-$ and $CD4^+CD25^+CD45RO^+$ T_{regs}.

3.1.2. The ratio between $CD4^+CD25^+CD45RO^-$ precursor and $CD4^+CD25^+CD45RO^+$ mature T_{regs} is inverted in early adulthood:

By analyzing cord and peripheral blood data for precursor $CD4^+CD25^+CD45RO^-$ and mature $CD4^+CD25^+CD45RO^+$ T_{regs}, we observe that their ratio is inverted before or in early adulthood. Indeed, in Fig. 5(C), we see from the experimental data giving the proportions of precursor and mature T_{regs} that there is a majority of precursors ($\sim 80\%$) in the cord blood of newborns and a majority of mature T_{regs} ($\sim 80\%$) in the peripheral blood of adult donors. This ratio is inverted at latest in the early adulthood (20–30 years of age) and this inversion is what we call the "development of an *in vivo* pool of $CD4^+CD25^+CD45RO^+$ mature T_{regs}". The following results show that the ratio inversion is a critical issue that is not achieved by all model scenarios.

3.2. Analysis of the mean model

In this section, we fit the mean model to the data of Fig. 5. As a reminder, the mean model is derived from the stochastic one by fixing the parameters of group G_1 to the mean value of their *a priori* distribution and by averaging over the remaining random quantities.

Fig. 6 shows the trajectories of precursors (left subplots) and mature T_{regs} (right subplots) under the four proliferation scenarios. Parameters h_P, h_Q, λ, φ_P, φ_Q, Q_M, α, p_{thymus} and s are fitted to the data using a least squares procedure (see Table 4 for best-fit values and Table S1 of the Supplementary Material for confidence intervals). The three different line types and colors in Fig. 6 correspond to the three homeostasis scenarios: solid red, scenario (i) (density-independent regulation), dashed blue, scenario (ii) (density-dependent regulation) and dash-dotted green, scenario (iii) (external contribution). The dynamics of precursors are very similar for all scenarios: we observe an increase during the first 10 years, followed by an exponential decrease. This is not surprising as this population is mainly influenced by the influx of recent thymic emigrants. The major difference is in the dynamics of mature T_{regs}. This population increases constantly with age, but according to the studied scenario, we observe qualitative differences in the way the population grows.

Before assessing the proliferation scenarios, we first wanted to see whether one or the other homeostasis scenario is better

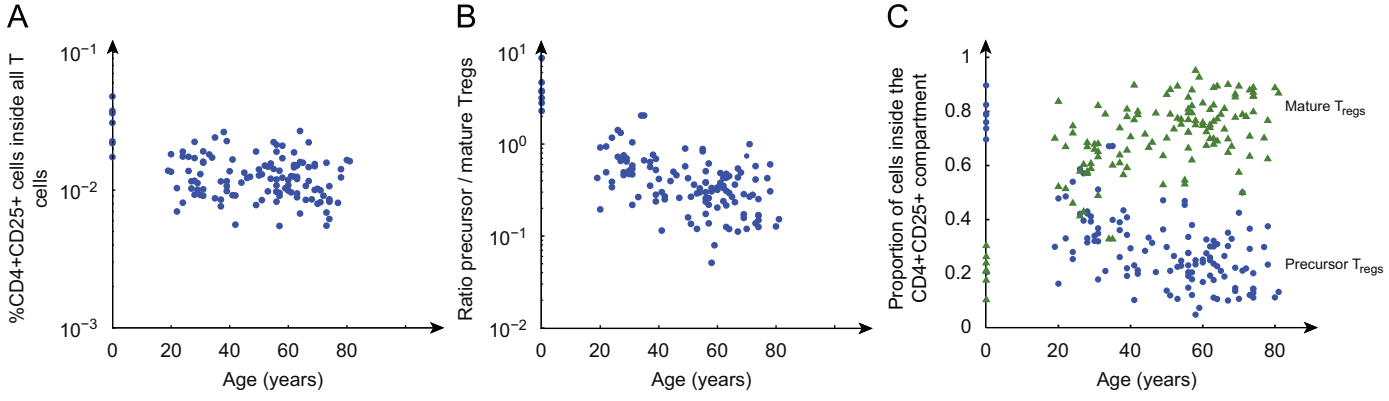

Fig. 5. Immunological data and properties of T_{regs} dynamics. (A) % $CD4^+CD25^+$ cells inside all T cells; (B) ratio $CD4^+CD25^+CD45RO^-$ precursor/$CD4^+CD25^+CD45RO^+$ mature T_{regs} as a function of age; (C) the ratio between precursor and mature T_{regs} is inverted in early adulthood.

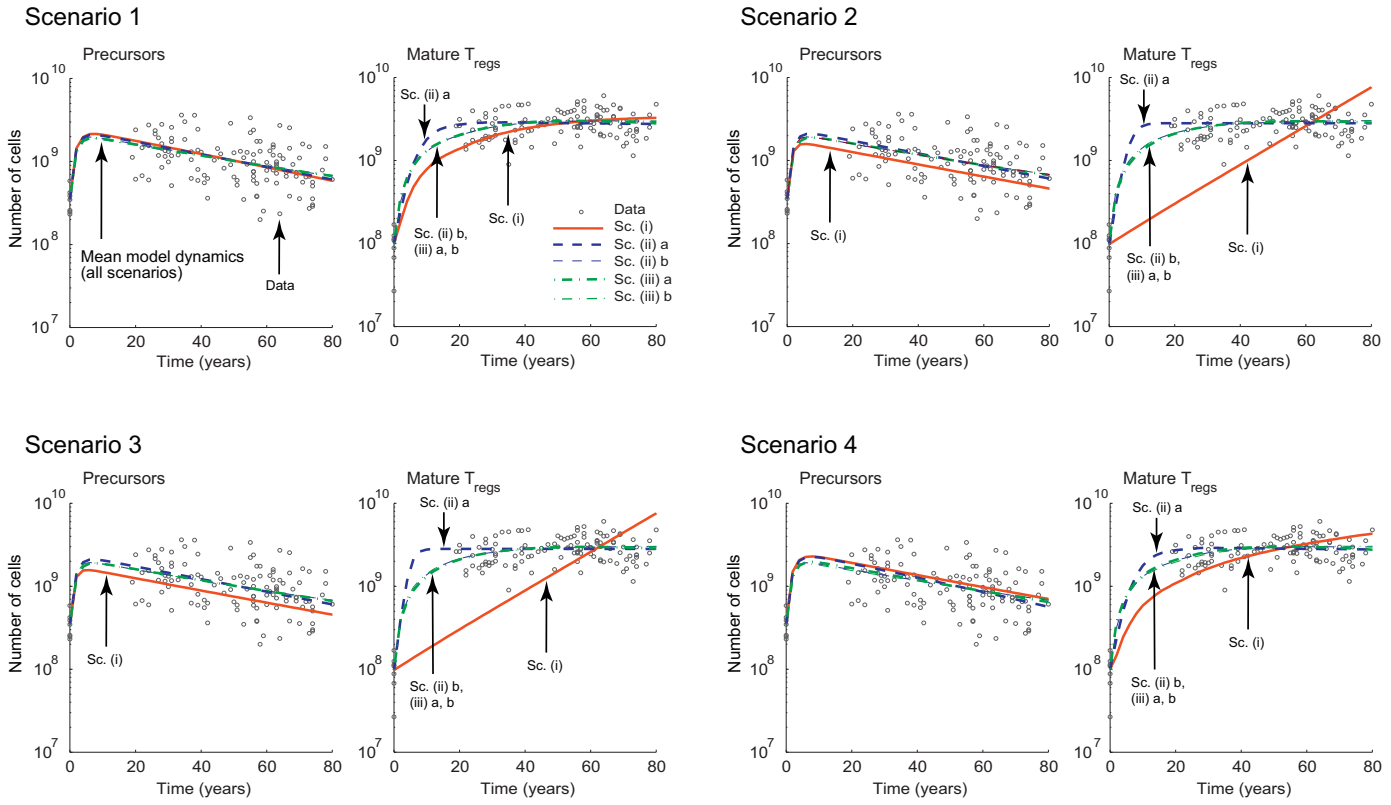

Fig. 6. Best-fit of the mean model with parameters of group G_1 set to the mean values of their *a priori* distributions. Solid red: for scenario (i) (density-independent regulation); dashed blue: scenario (ii) (density-dependent regulation) and dash-dotted green: scenario (iii) (external contribution). Bold lines: sub-setting (a), light lines: sub-setting (b). The ratio inversion between precursor and mature T_{regs} is not achieved early enough in scenarios 2(i) and 3(i). All other scenarios are able to explain the data. (For interpretation of the references to color in this figure legend, the reader is referred to the web version of this article.)

Table 4
Best-fit parameters of the mean model dynamics for each model scenario.

Scenario	Best-fit parameters								
	h_P ($\times 10^{-5}$ day^{-1})	h_Q ($\times 10^{-5}$ day^{-1})	λ (days)	φ_P ($\times 10^{-13}$ day^{-1} cell^{-1})	φ_Q ($\times 10^{-13}$ day^{-1} cell^{-1})	Q_M ($\times 10^7$ cells)	α (day^{-1})	p_{thymus} (%)	s ($\times 10^5$ cells)
1 (i)	−7.83	−8.87	51.65	4.86					
(ii) a	−4.42	60.53	58.98	3.27	2.54				
(ii) b	7.84	−18.20	99.44	4.41		7.50	0.0051		
(iii) a	7.10	−8.05	92.94	3.84				83.95	
(iii) b	14.35	−16.74	95.37	5.11					3.23
2 (i)	−0.48	15.16	0.95	6.36					
(ii) a	−4.69	156.40	60.88	3.23	5.55				
(ii) b	12.19	−16.61	164.80	4.87		2.04	0.0250		
(iii) a	6.54	−1.78	100.95	3.63				78.87	
(iii) b	12.22	−16.21	97.34	4.87					4.96
3 (i)	−0.29	15.07	1.25	6.50					
(ii) a	−4.75	203.77	55.39	3.22	7.23				
(ii) b	12.00	−17.35	168.80	4.85		6.02	0.0090		
(iii) a	6.55	−1.78	101.74	3.63				78.87	
(iii) b	12.52	−16.18	98.47	4.90					4.95
4 (i)	−20.53	−5.97	63.57	1.48					
(ii) a	−13.78	64.60	55.70	2.29	2.66				
(ii) b	12.15	−19.96	98.57	4.87		9.90	0.0045		
(iii) a	2.29	−7.96	91.78	3.29				81.87	
(iii) b	17.46	−16.98	92.24	5.42					3.43

explaining the data. For this, we applied an F-test for nested models opposing consecutively scenario 1(i) (H_0) to scenarios 1(ii)a, 1(ii)b, 1(iii)a and 1(iii)b (H_1). At level 0.01, H_0 was *not* rejected. This suggests that we do not have a strong evidence that a density-dependent homeostatic mechanism is regulating the population of mature T_{regs}.

The following three subsections describe the assessment results of the four proliferation scenarios, given either homeostasis scenario (i), (ii), or (iii).

3.2.1. In the case of a density-independent regulation of mature T_{regs}, the ratio inversion is a critical issue if the peripheral differentiation of precursors is the unique source of mature T_{regs}:

First note that due to the linearity of the differential equations of scenario (i), the ratio inversion can be achieved either because of a lifespan difference or through the slow accumulation of mature T_{regs} following an immune response. In what follows, we will see that the lifespan difference alone is not sufficient to achieve the ratio inversion.

From the solid red lines of the upper plots in Fig. 6, we see that scenario 1(i) is achieving the ratio inversion, whereas scenario 2(i) is not. The difference between these two scenarios is easy to explain when observing the typical trajectories of P, Q and R in Fig. 4. Indeed, the magnitude of immune responses is very different in both scenarios (zoomed sections of Fig. 4). In scenario 1(i), the clonal expansion goes up to 10^7 cells, whereas in scenario 2(i), it does not exceed 10^5 cells. This has an impact on the size of the mature T_{regs} pool: in the case of scenario 2(i), the only input to the mature T_{regs} population are the long-lived cells that have survived an immune reaction and they are set as 10% of the maximum effector response. As the peak of the effector response is relatively low, caused by the non-proliferating state of T_{regs} in scenario 2(i), very few cells feed the mature T_{regs} pool. Therefore, in scenario 2, the only way to achieve a ratio inversion is through a difference in parameters h_P and h_Q, because there is a deficient accumulation of mature T_{regs} following an antigen response. The latter parameters being fitted, we see that scenario 2(i), even with positive values of h_Q (Table 4) cannot reach the plateau level of the pool of mature T_{regs} suggested by the data. This suggests that, in the case of a density-independent regulation of mature T_{regs}, the slow accumulation observed only when there is a sufficient population expansion during antigen-triggered immune reactions is necessary to achieve the ratio inversion.

A similar explanation is valid for scenario 3(i) in which only precursors are endowed with a proliferation capacity. This scenario seems to be unable to accumulate a sufficient pool of mature T_{regs} (bottom left subplot of Fig. 6). This is because for the mean values of the parameters of group G_1 (Table S0 in Supplementary Material), the differentiation rate b is on average larger than the proliferation rate a_P, meaning that following an antigen priming, precursors have a higher probability of differentiating into hyporesponsive mature T_{regs} than to proliferate as precursors. Thus, most cells become anergic before having divided and the mature T_{regs} pool is underfed. As in scenario 2(i), a large and positive h_Q (Table 4) is not able to make up for the lack of accumulation of mature T_{regs} following antigen priming. In order to eliminate any dependence of this result to the exact values of the parameters of group G_1, we will study the behavior of scenario 3(i) in the stochastic model (Section 3.3).

Finally, the analysis of the mean model trajectory for scenario 4(i) suggests that the ratio can be inverted (bottom right subplot of Fig. 6). Note that this scenario is favored by the fact that the rate of secondary infections increases with age. Secondary responses recruit more mature T_{regs} that, once activated, start proliferating intensively. Therefore, the fact that precursors do not divide has only a minor impact on the population dynamics. However, we will evaluate the performance of this scenario with the stochastic model in order to see how it is affected by a change in the proliferation parameter values.

3.2.2. In the presence of a density-dependent homeostatic regulation of mature T_{regs}, the ratio precursor/mature T_{regs} is inverted without the need of peripheral proliferation in response to antigens:

This claim is suggested by the best-fit of homeostasis scenario (ii), where the population size is regulated either via a density-dependent death (sub-setting (a), bold dashed lines in Fig. 6), or via a density-dependent homeostatic proliferation (sub-setting (b), light dashed lines in Fig. 6). We see that both mechanisms produce different dynamics, but the lack of data in the age-range 0–19 years does not allow us to eliminate either of them. The sum of squared errors indicates however that a density-dependent homeostatic renewal (scenario 1(ii)b) fits slightly better the data. This is not surprising as this scenario has one more parameter than scenario 1(ii)a.

It is interesting to observe that a density-dependent death compensates for a large and positive value of h_Q (Table 4) meaning that the turnover rate of the mature T_{regs} population is very high. Concerning the density-dependant homeostatic renewal, we see from Table 4 that the per cell maximal renewal rate α needs to be on average 2 times larger in the case of hyporesponsiveness to antigen stimulation (scenario 2(ii)b) compared to the case where cells proliferate (scenario 1(ii)b). Therefore we conclude that the density-dependent regulation is able to explain the data, as long as there are no restrictions in the parameters defining the homeostatic proliferation and death rates.

3.2.3. The ratio inversion is easy to achieve without peripheral proliferation if there is an exponentially decreasing thymic output or a constant external input to the mature T_{regs} population:

This can be seen by analyzing the performance of homeostasis scenarios (iii)a and b. The green dash-dotted lines in Fig. 6 show the best-fit of these scenarios to the data (bold: scenario (iii)a, thymic output of mature T_{regs}; light: scenario (iii)b, external source). The ratio precursors/mature T_{regs} is inverted regardless the underlying proliferation scenario. Although there is no density-dependent regulation here, the increase of the population of mature T_{regs} is due to the thymic output of mature T_{regs} (scenarios 1–4(iii)a) or to the external and constant input of mature T_{regs} (scenarios 1–4(iii)b) from a phenotype switching of $CD4^+CD25^-$ T cells. Thus, we conclude that in this case, the peripheral proliferation of precursor or mature T_{regs} is not required for the development of the mature T_{regs} pool.

Furthermore, by analyzing the best-fit parameters of scenarios 1–4(ii)a (Table 4), we see that on average, the estimated value of p_{thymus} is about 80%. This means that the data can be explained with 20% of all $CD4^+CD25^+$ T cells that exit the thymus having a $CD45RO^+$ mature profile. Assuming that there are 1.3% $CD4^+CD25^+$ T_{regs} inside all $CD4^+$ T cells exiting the thymus, 20% (mature T_{regs}) of all T_{regs} is equivalent to 0.26% of all $CD4^+$ T cells. Thus, if as few as 0.26% of all $CD4^+$ T cells exiting the thymus are mature T_{regs}, antigen-driven proliferation in periphery is no longer necessary for the deployment of the pool.

3.3. Analysis of the stochastic model

The analysis of the mean model led to the rejection of model scenarios 2(i) and 3(i). However, this is true for the mean values of the *a priori* distributions, but it might not be true for all parameter values. To eliminate this possibility, we fit the stochastic model with parameters of group G_1 sampled from the distributions in Table S0. We apply this only to homeostasis scenario (i), as the other homeostasis scenarios were able to explain the data already with the mean model.

In order to obtain results that are robust with respect to parameter values, we define three parameter settings (Table 5)

that give slightly different results. These settings concern three important parameters of the immune response: a_P, the proliferation rate of precursors, a_R, the proliferation rate of activated mature T_{regs} and b, the differentiation rate of precursors into mature T_{regs}. In the first parameter setting of Table 5, the average value of b is larger than the average value of a_P, in other words, precursors have a higher probability of acquiring the mature phenotype than to proliferate as precursors in response to a foreign antigen. In settings 2 and 3, it is the opposite: precursors stay longer (and possibly proliferate) in this undifferentiated state before acquiring the mature phenotype. In settings 1 and 2, a_R takes values 1.4 times smaller than the values of a_P as measured *in vitro*, whereas in setting 3, we model an extreme case where mature T_{regs} proliferate, but 5 times less than precursors. Note that the analysis of the mean model in Section 3.2 was done under parameter setting 1.

To give an idea of the spread of trajectories of the stochastic model, Fig. 7 shows the best-fit of the stochastic model under scenarios 1–4(i) (parameter setting 1). In what follows, we use the evaluation procedure described in the Methods to assess all proliferation scenarios and find those that are unable to explain the biological data.

Table 5
Parameter values and distributions of the three parameter settings.

	$\mathbf{a_P}$ (day^{-1})	$\mathbf{a_R}$ (day^{-1})	$\mathbf{b}$ (day^{-1})
Parameter setting 1	$U(1, 2)$	$a_R = a_P/1.4$	$U(1, 10)$
Parameter setting 2	$U(1, 2)$	$a_R = a_P/1.4$	$U(0.5, 1)$
Parameter setting 3	$U(1, 2)$	$a_R = a_P/5.0$	$U(0.5, 1)$

$U(a,b)$ stands for a uniform distribution on $[a,b]$.

3.3.1. *In the absence of a density-dependent homeostatic regulation and of an external source of CD4$^+$CD25$^+$CD45RO$^+$ mature T_{regs}, proliferation of precursors or of mature T_{regs} is necessary to the development of the mature T_{regs} pool:*

This result is obtained in the case where the unique source of mature T_{regs} is the peripheral differentiation of precursors without density-dependent homeostatic regulation (scenario (i)). The results of the model evaluation procedure applied to the four proliferation scenarios are shown in Fig. 8A (see Table S2 of the online Supplementary Material for the best-fit parameters of the stochastic model). Each bar of Fig. 8 indicates the absolute value of the maximum likelihood of a proliferation scenario. The closer this bar is to zero, the better the model is explaining the data.

We observe that scenario 2(i), i.e., the one in which neither precursors nor mature T_{regs} proliferate, has a very poor performance in all three settings of Table 5. As stated in the previous section, the problem with this scenario is its inability to achieve the ratio inversion. Indeed, we found no parameter values such that this scenario is explaining the data. Scenario 2(i) is therefore rejected when compared to scenario 1(i) using the F-test for nested models (in all parameter settings). This implies that the proliferation of precursors and of mature T_{regs} following a successful interaction with an antigen presenting cell is essential

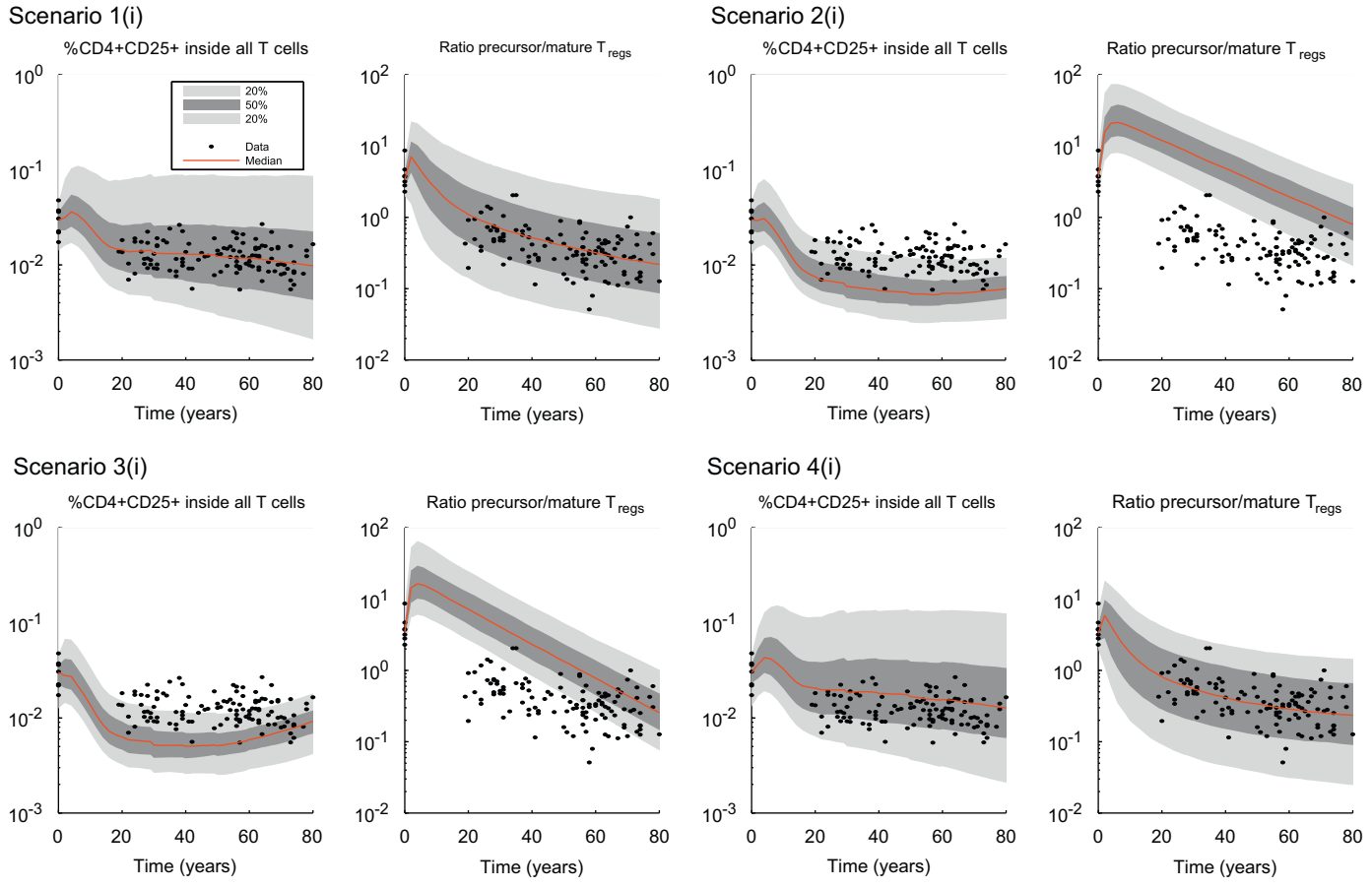

Fig. 7. Distribution of model's trajectories for scenarios 1(i)–4(i), parameter setting 1, fitted to the data. As the parameters are drawn from probabilistic distributions, every execution of the dynamical system is performed with different parameter values and the trajectories differ. Therefore, instead of a single trajectory, we have a distribution of trajectories. Solid red line: median. Fifty percent of the trajectories are comprised between the 25% and 75% quantiles (dark grey zone); 40% of all trajectories are in the light grey zone, delimited by quantiles 5–25% and 75–95%. (For interpretation of the references to color in this figure legend, the reader is referred to the web version of this article.)

to the development of a stable pool of mature T_{regs} in the absence of a density-dependent homeostatic regulation and of an external source of $CD4^+CD25^+CD45RO^+$ regulatory T cells.

Now, in order to test which proliferating capacity is more important, the one of precursors or the one of mature T_{regs}, we fit the stochastic model scenarios 3(i) and 4(i).

3.3.2. The proliferation of precursors alone is sufficient if $\mathbb{E}[b] < \mathbb{E}[a_P]$:

Fig. 8A shows the results of the evaluation procedure applied to scenario 3(i) (light grey bars) in which only precursors are endowed with a proliferation capacity. We remark that, as suggested by the assessment of the mean model, this scenario performs poorly in parameter setting 1. However, using the stochastic model, we have found two other parameter settings (2 and 3) for which scenario 3(i) performs similarly to scenario 1(i). Thus, the stochastic model suggests that there exist parameter values for which the proliferation of precursors alone is sufficient to the development of a viable pool of mature T_{regs}. As a consequence, the F-test for nested models rejects scenario 3(i) only in parameter setting 1. The difference between parameter setting 1 and parameter settings 2 and 3 being in the average value of the differentiation rate b with respect to the value of the proliferation rate of precursors a_P, we conclude that in order to validate model scenario 3(i), it must be shown that the proliferation rate a_P of precursor cells is significantly larger than the rate b of expression of CD45RO following an antigen stimulus.

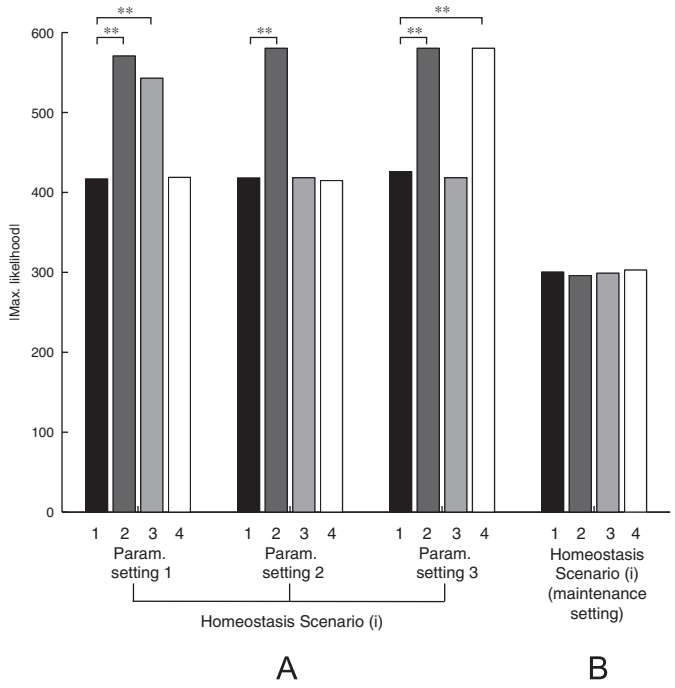

Fig. 8. Goodness of fit of the mathematical model in scenario (i) (no homeostatic regulation). The bar plot shows the absolute value of the log-likelihood of each model scenario. (black bars: proliferation scenario 1, dark grey: prolif. scenario 2, light grey: prolif. scenario 3, white: prolif. scenario 4). The closer the bar is to zero, the better the model fits the data. For each homeostasis scenario, we compare proliferation scenario 1 to all the others by applying a hypothesis test for nested models. A significant difference indicated by ** ($p-$value < 0.01) means that the considered scenario is rejected.

3.3.3. The proliferation of mature T_{regs} alone is sufficient if their division rate is not too small compared to the division rate of precursors:

The assessment of model scenario 4(i) in which only mature T_{regs} proliferate is illustrated in Fig. 8A (white bars). For settings 1 and 2, the performance of this scenario is comparable to the one of scenario 1(i), whereas for parameter setting 3, scenario 4(i) is not able to reproduce the dynamics of the data and the maximum likelihood is fairly low. In that case, the F-test for nested models rejects scenario 4(i) when compared to scenario 1(i). We remark that this happens in the extreme case where mature T_{regs} proliferate very little (the distribution of a_R in parameter setting 3 is $\mathcal{U}(1/5,1.7/5)$). Thus, the proliferation of mature T_{regs} is sufficient for the development of a peripheral pool only if the proliferation rate is not too small.

3.4. Maintenance of a lifelong in vivo pool of $CD4^+CD25^+CD45RO^+$ mature T_{regs}

In order to assess the importance of antigen-driven proliferation in the lifelong maintenance of a peripheral pool of T_{regs}, we examine the situation where the model is executed from the time at which the pool is already constituted, i.e., from the age corresponding to our first adulthood data (19 years old). We only study here homeostasis scenario (i), as it is the only one that led to the rejection of some proliferation scenarios.

Table 6
Summary of all our findings.

Biological process	Findings	Found using the…
Properties of T_{regs} dynamics	1. Homeostasis is maintained over both $CD4^+CD25^+CD45RO^-$ precursor and $CD4^+CD25^+CD45RO^+$ mature T_{regs} populations	Data
	2. The ratio between $CD4^+CD25^+CD45RO^-$ precursor and $CD4^+CD25^+CD45RO^+$ mature T_{regs} is inverted in early adulthood	Data
Development of the mature T_{regs} pool	3. The inversion of the ratio precursor/mature T_{regs} is easy to achieve in the presence of a density-dependent homeostatic mechanism of the mature T_{regs} population. In this case, there is no need of proliferation in response to immunogen stimulation	Model
	4. The ratio inversion is easy to achieve if there is a thymic or a constant external input to the mature T_{regs} population	Model
	5. In the absence of a density-dependent homeostatic regulation and of an external source of $CD4^+CD25^+CD45RO^+$ mature T_{regs}, proliferation of precursors or of mature T_{regs} is necessary to the development of the mature T_{regs} pool	Model
	6. The proliferation of precursors alone is sufficient if the proliferation rate of precursors is significantly larger than the rate of expression of CD45RO following an immunogen stimulus	Model
	7. The proliferation of mature T_{regs} alone is sufficient if their division rate is not too small compared to the division rate of precursors	Model
Maintenance of the mature T_{regs} pool	8. Given that at the age of 20 a peripheral pool of mature T_{regs} is constituted, antigen-driven proliferation in the periphery is not necessary for the maintenance even in the absence of other input of mature T_{regs} or of a density-dependent homeostasis mechanism	Model

Given that at the age of 20, *a peripheral pool of mature* T_{regs} *is constituted, antigen-driven proliferation in the periphery is not necessary for the maintenance even in the absence of other input of mature* T_{regs} *or of a density-dependent homeostasis mechanism*: We assess the four proliferation scenarios of Table 3, in the case of homeostasis scenario (i). The percentage of precursors inside $CD4^+CD25^+$ T cells at the age of 19 (p_{19}) is drawn from a Gaussian distribution with mean 0.35 and standard deviation 0.1, values obtained from the statistics of the data points corresponding to the age range 19–24 years. The percentage of mature T_{regs} at the age of 19 is set to $1-p_{19}$. The maximum likelihood of the fit of the stochastic model under all proliferation scenarios is in Fig. 8B. None of the scenarios is rejected after the likelihood ratio test. Thus, the proliferation in response to antigen stimuli is not necessary for the lifelong maintenance of a pool of mature T_{regs}, once the pool is constituted (Table 6).

A summary of all our findings can be found in Table 6.

4. Discussion

With the help of a mathematical model, we studied different developmental pathways of regulatory T cells and established conditions in which each of them can explain the biological data. The stochastic infection process combined with the differential equations with random parameters and Monte Carlo simulation is a modeling methodology allowing the description of cell dynamics on the scale of years. We believe that such a scheme is particularly appropriate for use in human studies, where data are sparse and several sources of uncertainty and noise have an influence on parameter values. Although still requiring the computation of confidence intervals, using random parameters was a way of avoiding tedious high-dimensional parameter fitting by decreasing the number of unknown parameters and instead, introducing distributions covering an entire set of possible values. In order to keep the model tractable, we have made several simplifying assumptions. One of them is the assumption that, except for thymic involution, parameter distributions are independent on age. This is probably a simplification, but recent studies indicate that $CD4^+CD25^+$ T_{regs} in aged mice are functionally comparable to those in young mice (Nishioka et al., 2006).

In an effort to keep the model simple, we used a two-phase model (Eqs. (1) and (2)) that describes the way cells respond to antigen stimulus when only the responder cell population is considered (De Boer et al., 2003; Althaus et al., 2007). Such a model corresponds to a view of the immune system where the size of immune responses is proportional to the number of pre-existing cells. However, the biological reality might be more complicated and it could be possible that the number of cells produced at the end of an immune response is independent of the initial number of cells.

We have observed that the number of $CD4^+CD25^+CD45RO^-$ precursor T_{regs} decreases with age. This result confirms the findings of Valmori et al. (2005), where the authors point out a significant negative correlation between the number of precursors and the age of donors. Then, we have observed that the number of $CD4^+CD25^+CD45RO^+$ mature T_{regs} increases with age. This finding as well goes in the direction of the results of Valmori et al. (2005) and is in accordance with the results of Gregg et al. (2005), where the authors observe an increased number of peripheral $CD4^+CD25^{hi}$ T cells. We then have shown that the ratio between precursors and mature T_{regs} is inverted in early adulthood. Furthermore, the model suggested the continuous-time trajectory of T_{regs}. In particular, we have observed interesting cell dynamics during infancy and puberty, time-periods for which we have not found immunological data due to ethical reasons. As this is the period of life where the thymus functions at a maximal regime, we have observed an important increase of thymus-derived precursor cells, peaking at 10–12 years old, age corresponding to the onset of puberty. Then, precursor cells start their decline, while mature T_{regs} continue their progressive increase, having their most important increase rate in the age range 0–20 years. The latter is thus a critical period for the constitution of a pool of mature T_{regs}. This ratio inversion was also a critical issue of the model behavior; it led to the elimination of some model scenarios that could not reproduce it.

We have studied several pool-size regulation mechanisms of T_{regs}: density-independent and density-dependent renewal/death of mature T_{regs}, as well as a constant or time-dependent external contribution. Given these distinct mechanisms, we have identified conditions in which the antigen-driven proliferation is necessary for the creation of a viable pool of $CD4^+CD25^+CD45RO^+$ T_{regs}. It turned out that the antigen-driven proliferation is not necessary if a density-dependent homeostatic mechanism regulates the pool of mature T_{regs}. In other terms, as we found no information about the exact values of the parameters governing the homeostatic regulation, the antigen-driven cell division could be replaced in our model by a homeostatic (cytokine-driven) proliferation. However, the homeostatic expansion is unlikely to be the main source of mature T_{regs}, because if that was the case, the diversity of the T cell receptor (TCR) repertoire would be reduced by competitive exclusion. Indeed, if there is no external contribution to this cell population, the diversity of T cell receptors would be determined by the few cells present at birth. Yet, it is known that T_{regs} have an $\alpha\beta$ TCR repertoire with size and diversity closely similar to those of $CD4^+CD25^-$ T cells (Fazilleau et al., 2007). Therefore, we believe that in addition to a homeostatic mechanism, other sources of *de novo* generation should be present.

In this perspective, we have studied other sources of mature T_{regs} that are able to replenish the peripheral pool of mature $CD4^+CD25^+CD45RO^+$ T_{regs} and enrich the TCR repertoire. One such source is the thymus output of mature T_{regs}. We have established the percentage of T_{regs} that should be output daily from the thymus so that the peripheral expansion of this population is not required for a successful development of the pool. This threshold is about 20% of all $CD4^+CD25^+$ T cells output from the thymus, or, equivalently, less than 0.3% of all $CD4^+$ T cells exiting the thymus. Another question arises then: Are T_{regs} with a mature phenotype able to exit the thymus? We found two points of view in the literature.

On the one hand, Wing et al. (2003) claim that only regulatory T cells with a naive phenotype, namely $CD45RO^-$ precursors, are released in the periphery from the thymus (corresponding to our homeostasis scenario (i)). If this is indeed the case, then we have demonstrated that proliferation of both $CD4^+CD25^+CD45RO^-$ and $CD4^+CD25^+CD45RO^+$ cells is sufficient, but not necessary for the development and maintenance of a pool of T_{regs}. In scenario 3(i), where only precursors proliferate, we saw that if the differentiation rate of $CD4^+CD25^+CD45RO^-$ precursors into $CD4^+CD25^+CD45RO^+$ mature T_{regs} is similar to or greater than the proliferation rate of precursors, the model cannot explain the data. However, it is unlikely that precursor cells stop suddenly their proliferation because of the acquisition of the mature phenotype. Our *in vitro* experiments have shown that in presence of antigen with a co-stimulatory signal, precursor $CD4^+CD25^+$ $CD45RO^-$ cells proliferate intensively while acquiring the memory phenotype (unpublished data). This observation suggests that either the acquisition of CD45RO is not associated with anergy during a first priming, in which case, instead of scenario 3(i), scenario 1(i) would be the appropriate model, or the parameters governing cell dynamics have the property that the rate of proliferation of precursors is greater than the rate of differentiation

into mature T_{regs}, in which case scenario 3(i) is in accordance with the *in vivo* data. In scenario 4(i), where only activated recently-matured $CD4^+CD25^+CD45RO^+$ cells proliferate, cells start their intense proliferation after a time-delay, which is compatible with the fact that regulatory T cells activate slowly, only when there is a sufficient amount of growth resources in the environment. The fact that the expansion of regulatory T cells is dependent on growth factors produced by other cells was also pointed out in Leon et al. (2000) and Burroughs et al. (2006). A recent study (Lee et al., 2008) brings light to the molecular mechanisms through which Foxp3 maintains the unresponsiveness of T_{regs}. The link of Foxp3 to c-Jun blocks proliferation and therefore makes it even more difficult for T_{regs} to activate and proliferate. Scenario 4 with its initial delay, attests for this difficulty.

On the other hand, it cannot be excluded that a small proportion of mature-type T_{regs} might exit thymus tissues. Vanhecke et al. (1995) identify five stages of thymocyte differentiation during which $CD4^+$ T cells acquire and lose several surface receptors. The last two stages define the most mature cells that consist of $CD4^+CD1^-CD45RO^+$ (stage 4) and $CD45RO^-$ (stage 5) helper T cells. As no particular sorting was applied to mark regulatory T cells in this study, we can assume that they are comprised in the above populations. Vanhecke et al. (1995) claim that both stage 4 and stage 5 cells emigrate from the thymus in a severe combined immunodeficient mouse carrying a human thymus, even though they consider $CD45RO^-$ stage 5 cells as more mature. Another question arises then, which is whether these thymic emigrants with mature profile switch back to a naive form soon after their entry in the periphery or not. This event was not considered in our mathematical model, but it will certainly reinforce the need of proliferating capacity of T_{regs} for the development of a reliable pool. However, if these stage 4 $CD45RO^+$ T_{regs} maintain the mature profile once in the periphery, their number could be sufficient for the development of a pool of mature T_{regs}.

Recent studies point out the presence of an input of mature T_{regs} coming from non-regulatory helper T cells (Vukmanovic-Stejic et al., 2006). This hypothesis is perfectly able to explain the biological data, when daily there are at least 10^5 $CD4^+CD25^-$ cells acquiring a regulatory profile. To our knowledge, there is no quantitative data measuring this transformation, nonetheless, we hypothesize that this external contribution should be such that the entire pool of $CD4^+CD25^+FoxP3^+$ cells, including naturally occurring thymus-derived T_{regs}, is in steady state, as suggested by our data.

At last, we have shown that although the antigen-driven proliferation of regulatory T cells is essential for the development of a pool of mature T_{regs}, it is not a critical issue for the lifelong maintenance of this compartment. This finding confirms the intuitive fact that the homeostasis-related kinetics have more impact on the lifelong maintenance of a cell population than the antigen-response kinetics.

An important contribution of the mathematical model described here is the suggestion of new research directions that will deepen our knowledge about regulatory T cells. Indeed, our results led to the identification of crucial mechanisms having an important impact on T_{regs} dynamics and that could be subject to further investigations: the quantitative assessment of the parameters governing the homeostatic maintenance of T_{regs}, the assessment of the quantity of mature T_{regs} exiting the thymus, and the quantitative description of the phenomena transforming a non-regulatory cell into a regulatory $CD4^+CD25^+FoxP3^+$ T cell *in vivo*.

In conclusion, the mathematical model allowed us to have a global view on the lifelong dynamics of T_{regs}. We evaluated three different homeostatic scenarios about possible sources of mature T_{regs} that can explain how a stable pool of T_{regs} is developed and maintained through human life. This enabled us to appreciate and estimate the different contributions of each single path in the absence of others. Moreover, we also evaluated four different scenarios concerning the intrinsic proliferation ability of precursors and mature T_{regs}. This ability has a considerable impact on T_{regs} development and maintenance if precursors are the unique source of mature T_{regs}. Our model is the first attempt to mathematically and computationally describe the behavior of regulatory T cells over life. The mathematical model is able to estimate the trend of T_{regs} over time when one or more sources are affected. Although it is already possible to have an empirical idea of the future trend of regulatory T cells from the blood of a patient, it is not possible to predict their amount at a certain time in the future. Further developments could enable our *in silico* model to virtually monitor and predict the dynamics of regulatory T cells throughout an individual life. This application can be particularly useful for prospective studies on patients that received a solid organ transplant or are suffering from an autoimmune disease. Such patients have often decreased numbers of T_{regs} in their blood, compared to healthy donors. Once the mathematical model is able to predict the amount of T_{regs} over time, it would allow for the individual dosing of the immunosuppressive drugs needed to prevent chronic rejection episodes or disease relapses. In the perspective of introduction of regulatory T cells in cell-therapy as a more specific and sophisticated substitute to immunosuppressive drugs (Riley et al., 2009), our model is a first step towards the development of tools aiming at the clinical monitoring of regulatory T cell dynamics before and after their adoptive transfer.

Acknowledgment

The authors would like to thank Jean-Pierre Kraehenbuhl for his advice and useful discussions.

Appendix A. Supplementary data

Supplementary data associated with this article can be found in the online version at doi:10.1016/j.jtbi.2010.06.024.

References

Akbar, A.N., Vukmanovic-Stejic, M., Taams, L.S., Macallan, D.C., 2007. The dynamic co-evolution of memory and regulatory CD4+ T cells in the periphery. Nature Reviews Immunology 7 (March), 231–237.

Althaus, C.L., Ganusov, V.V., De Boer, R.J., 2007. Dynamics of CD8+ T cell responses during acute and chronic lymphocytic choriomeningitis virus infection. Journal of Immunology 179 (5), 2944–2951.

Burroughs, N.J., Mendes de Oliveira, B.M.P., Adrego, P.A., 2006. Regulatory T cell adjustment of quorum growth thresholds and the control of local immune responses. Journal of Theoretical Biology 241 (1), 134–141.

Carneiro, J., Leon, K., Caramalho, I., van den Dool, C., Gardner, R., Oliveira, V., Bergman, M., Seplveda, N., Paixo, T., Faro, J., Demengeot, J., 2007. When three is not a crowd: a crossregulation model of the dynamics and repertoire selection of regulatory CD4+ T cells. Immunological Reviews 216, 48–68.

CDC, 1988–1994. NHANES survey. Online. URL 〈http://www.cdc.gov〉.

Clark, D., Boer, R.J.D., Wolthers, K., Miedema, F., 1999. T cell dynamics in HIV-1 infection. Advances in Immunology 73, 301–327. doi:10.1016/S0065-2776(08)60789-0.

Codarri, L., Vallotton, L., Ciuffreda, D., Venetz, J.-P., Garcia, M., Hadaya, K., Buhler, L., Rotman, S., Pascual, M., Pantaleo, G., 2007. Expansion and tissue infiltration of an allospecific CD4+CD25+CD45RO+IL-7Rα^{high} cell population in solid organ transplant recipients. Journal of Experimental Medicine 204 (7), 1533–1541.

Cupedo, T., Nagasawa, M., Weijer, K., Blom, B., Spits, H., 2005. Development and activation of regulatory T cells in the human fetus. European Journal of Immunology 35, 383–390.

Darrasse-Jeze, G., Deroubaix, S., Mouquet, H., Victora, G.D., Eisenreich, T., Yao, K.H., Masilamani, R.F., Dustin, M.L., Rudensky, A., Liu, K., Nussenzweig, M.C., 2009.

Feedback control of regulatory T cell homeostasis by dendritic cells in vivo. Journal of Experimental Medicine 206 (9), 1853–1862.
Davison, A., 2003. Statistical Models. Cambridge University Press.
De Boer, R., Homann, D., Perelson, A.S., 2003. Different dynamics of CD4+ and CD8+ T cell responses during and after acute lymphocytic choriomeningitis virus infection. Journal of Immunology 171, 3928–3935.
De Boer, R., Opera, M., Antia, R., Murali-Krishna, K., Ahmed, R., Perelson, A., 2001. Recruitment times, proliferation, and apoptosis rates during the CD8+ T-cell response to lymphocytic choriomeningitis virus. Journal of Virology 75 (22), 10663–10669.
Dutilh, B., De Boer, R., 2003. Decline in excision circles requires homeostatic renewal or homeostatic death of naive T cells. Journal of Theoretical Biology 224 (March), 351–358.
Fazilleau, N., Bachelez, H., Gougeon, M.L., Viguier, M., 2007. Cutting edge: size and diversity of CD4+CD25high FoxP3+ regulatory T cell repertoire in humans: evidence for similarities and partial overlapping with CD4+CD25- T cells. Journal of Immunology 179 (6), 3412–3416.
Feldschuh, J., Enson, Y., 1977. Prediction of the normal blood volume. Relation of blood volume to body habitus. Circulation 56 (4), 605–612.
Fontenot, J.D., Gavin, M.A., Rudensky, A.Y., 2003. Foxp3 programs the development and function of CD4+CD25+ regulatory T cells. Nature Immunology 4 (4), 330–336.
Fouchet, D., Regoes, R., 2008. A population dynamics analysis of the interaction between adaptive regulatory T cells and antigen presenting cells. PLoS One 3 (5), e2306.
Fritzsching, B., Oberle, N., Pauly, E., Geffers, R., Buer, J., Poschl, J., Krammer, P., Linderkamp, O., Suri-Payer, E., 2006. Naive regulatory T cells: a novel subpopulation defined by resistance toward CD95L-mediated cell death. Blood 108 (10), 3371–3378.
Gavin, M.A., Clarke, S.R., Negrou, E., Gallegos, A., Rudensky, A., 2002. Homeostasis and anergy of CD4(+)CD25(+) suppressor T cells in vivo. Nature Immunology 3 (1), 33–41.
Gregg, R., Smith, C.M., Clark, F.J., Dunnion, D., Khan, N., Chakraverty, R., Nayak, L., Moss, P.A., 2005. The number of human peripheral blood CD4+CD25high regulatory T cells increases with age. Clinical and Experimental Immunology 140 (3), 540–546.
Hoffmann, P., Eder, R., Boeld, T.J., Doser, K., Piseshka, B., Andreesen, R., Edinger, M., 2006. Only the CD45RA+ subpopulation of CD4+CD25high T cells gives rise to homogeneous regulatory T-cell lines upon in vitro expansion. Blood 108 (13), 4260–4267.
Hombach, A.A., Kofler, D., Hombach, A., Rappl, G., Abken, H., 2007. Effective proliferation of human regulatory T cells requires a strong costimulatory CD28 signal that cannot be substituted by IL-2. Journal of Immunology 179 (11), 7924–7931.
Hori, S., Nomura, T., Sakaguchi, S., 2003. Control of regulatory T cell development by the transcription factor Foxp3. Science 299, 1057–1061.
Jonuleit, H., Schmitt, E., Stassen, M., Tuettenberg, A., Knop, J., Enk, A.H., 2001. Identification and functional characterization of human CD4+CD25+ T cells with regulatory properties isolated from peripheral blood. Journal of Experimental Medicine 193 (11), 1285–1294.
Kasow, K.A., Chen, X., Knowles, J., Wichlan, D., Handgretinger, R., Riberdy, J.M., 2004. Human CD4+CD25+ regulatory T cells share equally complex and comparable repertoires with CD4+CD25-counterparts. Journal of Immunology 172 (10), 6123–6128.
Kim, J.M., Rasmussen, J.P., Rudensky, A.Y., 2007. Regulatory T cells prevent catastrophic autoimmunity throughout the lifespan of mice. Nature Immunology 8 (2), 191–197.
Klein, L., Khazaie, K., von Boehmer, H., 2003. In vivo dynamics of antigen-specific regulatory T cells not predicted from behavior in vitro. Proceedings of the National Academy of Sciences 100 (15), 8886–8891.
Kretschmer, K., Apostolou, I., Hawiger, D., Khazaie, K., Nussenzweig, M., von Boehmer, H., 2005. Inducing and expanding regulatory T cell populations by foreign antigen. Nature Immunology 6, 1219–1227.
Lee, S.-M., Gao, B., Fang, D., 2008. FoxP3 maintains Treg unresponsiveness by selectively inhibiting the promoter DNA-binding activity of AP-1. Blood 111 (7), 3599–3606.
Leon, K., Perez, R., Lage, A., Carneiro, J., 2000. Modelling T-cell-mediated suppression dependent on interactions in multicellular conjugates. Journal of Theoretical Biology 207 (2), 231–254.
Liu, W., Putnam, A.L., Xu-yu, Z., Szot, G.L., Lee, M.R., Zhu, S., Gottlieb, P.A., Kapranov, P., Gingeras, T.R., de St. Groth, B.F., Clayberger, C., Soper, D.M., Ziegler, S.F., Bluestone, J.A., 2006. CD127 expression inversely correlates with FoxP3 and suppressive function of human CD4+ T reg cells. Journal of Experimental Medicine 203 (7), 1701–1711.
Marušić, M., Turkalj-Kljajić, M., Petrovečki, M., Užarević, B., Rudolf, M., Batinić, D., Ugljen, R., Anić, D., Ćavar, Z., Jelić, I., Malenica, B., 1998. Indirect demonstration of the lifetime function of human thymus. Clinical and Experimental Immunology 111 (2), 450–456.
Nishioka, T., Shimizu, J., Iida, R., Yamazaki, S., Sakaguchi, S., 2006. CD4+CD25+Foxp3+ T cells and CD4+CD25-Foxp3+ T cells in aged mice. Journal of Immunology 176 (11), 6586–6593.
Riley, J.L., June, C.H., Blazar, B.R., 2009. Human *t* regulatory cell therapy: take a billion or so and call me in the morning. Immunity 30 (5), 656–665.
Sakaguchi, S., 2003. The origin of FoxP3-expressing CD4+ regulatory T cells: thymus or periphery. Journal of Clinical Investigation 112 (9), 1310–1312.
Sakaguchi, S., Sakaguchi, N., Asano, M., Itoh, M., Toda, M., 1995. Immunologic self-tolerance maintained by activated T cells expressing IL-2 receptor alpha-chains (CD25). Breakdown of a single mechanism of self-tolerance causes various autoimmune diseases. Journal of Immunology 155, 1151–1164.
Seddiki, N., Santner-Nanan, B., Martinson, J., Zaunders, J., Sasson, S., Landay, A., Solomon, M., Selby, W., Alexander, S.I., Nanan, R., Kelleher, A., de St. Groth, B.F., 2006a. Expression of interleukin (IL)-2 and IL-7 receptors discriminates between human regulatory and activated T cells. Journal of Experimental Medicine 203 (7), 1693–1700.
Seddiki, N., Santner-Nanan, B., Tangye, S.G., Alexander, S.I., Solomon, M., Lee, S., Nanan, R., de Saint Groth, B.F., 2006b. Persistence of naive CD45RA+ regulatory T cells in adult life. Blood 107 (7), 2830–2838.
Steinmann, G., Klaus, B., Muller-Hermelunk, H.-K., 1985. The involution of the aging human thymic epithelium is independent of puberty. Scandinavian Journal of Immunology 22, 563–575.
Taams, L., Smith, J., Rustin, M., Salmon, M., Poulter, L., Akbar, A., 2001. Human anergic/suppressive CD4+CD25+ T cells: a highly differentiated and apoptosis-prone population. European Journal of Immunology 31 (4), 1122–1131.
Takahashi, T., Kuniyasu, Y., Toda, M., Sakaguchi, N., Itoh, M., Iwata, M., Shimizu, J., Sakaguchi, S., 1998. Immunologic self-tolerance maintained by CD25+CD4+ naturally anergic and suppressive T cells: induction of autoimmune disease by breaking their anergic/suppressive state. International Immunology 10 (12), 1969–1980.
Takahata, Y., Nomura, A., Takada, H., Ohga, S., Furuno, K., Hikino, S., Nakayama, H., Sakaguchi, S., Hara, T., 2004. CD25+CD4+ T cells in human cord blood: an immunoregulatory subset with naive phenotype and specific expression of forkhead box p3 (Foxp3) gene. Experimental Hematology 32 (7), 622–629.
Valmori, D., Merlo, A., Souleimanian, N.E., Hesdorffer, C.S., Ayyoub, M., 2005. A peripheral circulating compartment of natural naive CD4+ Tregs. Journal of Clinical Investigation 115 (7), 1953–1962.
Vanhecke, D., Verhasselt, B., Debacker, V., Leclercq, G., Plum, J., Vandekerckhove, B., 1995. Differentiation to T helper cells in the thymus. Gradual acquisition of T helper cell function by CD3+CD4+ cells. Journal of Immunology 155 (10), 4711–4718.
Vukmanovic-Stejic, M., Zhang, Y., Cook, J.E., Fletcher, J.M., McQuaid, A., Masters, J.E., Rustin, M.H., Taams, L.S., Beverley, P.C., Macallan, D.C., Akbar, A.N., 2006. Human CD4+CD25hiFoxp3+ regulatory T cells are derived by rapid turnover of memory populations in vivo. Journal of Clinical Investigation 116 (9), 2423–2433.
Walker, M.R., Kasprowicz, D.J., Gersuk, V.H., Benard, A., Van Landeghen, M., Buckner, J.H., Ziegler, S.F., 2003. Induction of FoxP3 and acquisition of T regulatory activity by stimulated human CD4+CD25- T cells. Journal of Clinical Investigation 112 (9), 1437–1443.
Walker, S., Chodos, A., Eggena, M., Dooms, H., Abbas, A., 2003. Antigen-dependent proliferation of CD4+CD25+ regulatory T cells in vivo. Journal of Experimental Medicine 198 (2), 249–258.
WHO, 2009. Child growth standards. Online. URL 〈http://www.who.int/childgrowth/standards/weight_for_age〉.
Wing, K., Ekmark, A., Karlsson, H., Rudin, A., Suri-Payer, E., 2002. Characterization of Human CD25+ CD4+ T cells in thymus, cord and adult blood. Immunology 106, 190–199.
Wing, K., Lindgren, S., Kollberg, G., Lundgren, A., Harris, R., Rudin, A., Lundin, S., Suri-Payer, E., 2003. CD4 T cell activation by myelin oligodendrocyte glycoprotein is suppressed by adult but not cord blood CD25+ T cells. European Journal of Immunology 33 (3), 579–587.
Yamaguchi, T., Hirota, K., Nagahama, K., Ohkawa, K., Takahashi, T., Nomura, T., Sakaguchi, S., 2007. Control of immune responses by antigen-specific regulatory T cells expressing the folate receptor. Immunity 27, 145–159.